Neuroscience 169 (2010) 609–618

INHIBITION OF N-METHYL-D-ASPARTATE RECEPTOR ACTIVITY RESULTED IN ABERRANT NEURONAL MIGRATION CAUSED BY DELAYED MORPHOLOGICAL DEVELOPMENT IN THE MOUSE NEOCORTEX

S. UCHINO,[a1] T. HIRASAWA,[a,b1] H. TABATA,[c1] Y. GONDA,[a] C. WAGA,[a] Y. ONDO,[a] K. NAKAJIMA[c] AND S. KOHSAKA[a]*

[a]*Department of Neurochemistry, National Institute of Neuroscience, 4-1-1 Ogawahigashi, Kodaira-shi, Tokyo 187-8502, Japan*

[b]*Department of Epigenetic Medicine, Interdisciplinary Graduate School of Medicine and Engineering, University of Yamanashi, 1110 Shimokato, Chuo-shi, Yamanashi 409-3898, Japan*

[c]*Department of Anatomy, Keio University School of Medicine, 35 Shinano-machi, Shinjuku-ku, Tokyo 160-8582, Japan*

Abstract—Embryonic and neonatal neocortical neurons already express functional *N*-methyl-D-aspartate (NMDA) receptors before they form synapses. To elucidate the role of NMDA receptors in neuronal migration in the developing neocortex, we visualized radially migrating neurons by transferring the enhanced green fluorescent protein (EGFP) gene into the ventricular zone (VZ) of the mouse neocortex using *in utero* electroporation at E15.5. Two days later, we prepared neocortical slices and examined the EGFP-positive cells using time-lapse imaging in the presence of the NMDA receptor antagonist Cerestat. The EGFP-positive cells generated in the VZ in the control slices exhibited a multipolar morphology, but within several hours they became bipolar (with a leading process and an axon-like process) and migrated toward the pial surface. By contrast, many of the multipolar cells in the Cerestat-treated slices failed to extend either process and become bipolar, and frequently changed direction, although they ultimately reached their destination even after Cerestat-treatment. To identify the molecules responding for mediating NMDA signaling during neuronal migration and the changes in morphology observed above, we here focused on Src family kinases (SFKs), which mediate a variety of neuronal functions including migration and neurite extension. We discovered that the activity of Src and Fyn was reduced by Cerestat. These findings suggest that NMDA receptors are involved in neuronal migration and morphological changes into a bipolar shape, and in the activation of Src and Fyn in the developing neocortex.

Key words: development, corticogenesis, Src family kinases, NMDA receptor antagonist, *in utero* electroporation.

Neuronal migration is an important process in brain development. Newborn neurons are influenced by several factors that regulate their morphology, mobility, and destination during migration, and recent studies have shown that neurotransmitters, including glutamate and GABA, have a crucial modulatory effect on neuronal migration (Luján et al., 2005; Heng et al., 2007). For example, the granule cell migration in the cerebellum depends on the activity of *N*-methyl-D-aspartate (NMDA) receptors (Komuro and Rakic, 1993). NMDA receptor antagonists and $GABA_A$ receptor antagonists affect the morphology of the migrating neurons in the hippocampus in a manner that severely impairs neuronal migration (Manent et al., 2005). Neurons in the developing cerebral cortex migrate in one of two directions. The excitatory projection neurons generated near the ventricle move to the developing cortical plate (CP) through a radial mode of migration (Angevine and Sidman, 1961; Berry and Rogers, 1965; Rakic, 1972), whereas the GABA-containing interneurons originate in ganglionic eminences and enter the developing CP through a tangential mode of migration (Marin and Rubenstein, 2001; Nakajima, 2007). Interestingly, Yozu et al. (2008) found that a subpopulation of medial ganglionic eminence (MGE)-derived cells in the neocortex stopped migrating or changed their direction of migration in response to AMPA, but that neither MGE-derived cells migrating in the subcortical territory nor radially migrating cells in the neocortex were affected by exposure to AMPA. These results indicate that the activation of AMPA receptors directly affects tangential migration in the neocortex. While many studies, including our own previous study (Hirasawa et al., 2003), have shown that the inhibition of NMDA receptors with an antagonist suppresses radial migration (Behar et al., 1999; Hirai et al., 1999; Simonian and Herbison, 2001), Kihara et al. (2002) observed that the stimulation of NMDA receptors also inhibited radial migration. Since the investigators in all the above-mentioned studies used 5-bromo-2′-deoxyuridine (BrdU) or [^{3}H]thymidine pulse-labeling experiments to examine neuronal migration, providing conclusive evidence of NMDA receptor-mediated neuronal migration has been difficult since neuronal migration was never investigated directly.

In the present study, we visualized migrating neurons by transferring an enhanced green fluorescent protein (EGFP)-encoding plasmid into the ventricular zone (VZ) of the murine embryonic cerebrum using *in utero* electroporation and directly observed the migrating cells in living neocortical slices using time-lapse imaging. These time-

[1] These authors contributed equally.

*Correspondence to: S. Kohsaka, Department of Neurochemistry, National Institute of Neuroscience, 4-1-1 Ogawahigashi, Kodaira-shi, Tokyo 187-8502, Japan. Tel: +81-42-346-1711; fax: +81-42-346-1741.
E-mail address: kohsaka@ncnp.go.jp (S. Kohsaka).

Abbreviations: BrdU, 5-bromo-2′-deoxyuridine; BSA, bovine serum albumin; CP, cortical plate; EGFP, enhanced green fluorescent protein; FAK, focal adhesion kinase; IMZ, intermediate zone; MLA, methyllycaconitine; NMDA, N-methyl-D-aspartate; PBS, phosphate-buffered saline; SFKs, Src family kinases; TBS-T, tris-buffered saline containing 0.1% Tween20; VZ, ventricular zone.

0306-4522/10 $ - see front matter
doi:10.1016/j.neuroscience.2010.05.024

lapse observations revealed that the migratory profile during the inhibition of NMDA receptors differed considerably from the radial migration observed in the control mice. We also found that the activity of Src family kinases, including Src and Fyn, was significantly reduced after exposure to an NMDA antagonist. These results provided evidence that NMDA receptors play an important role in the radial migration that occurs in the developing neocortex.

EXPERIMENTAL PROCEDURES

Crl:CD-1 (ICR) mice (Clea Japan, Tokyo, Japan) were used in this study. All experimental procedures were approved by The Animal Care and Use Committee of the National Institute of Neuroscience.

Gene transfer using in utero electroporation

Gene transfer using *in utero* electroporation was performed as previously described (Nakahira and Yuasa, 2005), but with a slight modification of the original procedures (Tabata and Nakajima, 2001). On embryonic day (E) 15.5 pregnant ICR mice were deeply anesthetized with diethyl ether (Wako, Osaka, Japan), and their uterine horns were exposed. Plasmid DNA pCAGGS-EGFP that had been purified using the CsCl/Ethidium Bromide equilibrium density-gradient centrifugation method was dissolved to a final concentration of 5 μg/μL in phosphate-buffered saline (PBS) and 0.05% Fast Green. Approximately 1–2 μL of the plasmid DNA solution was injected into a lateral ventricle of each embryo with a glass micropipette prepared from a microcapillary tube (GD-1; Narishige, Tokyo, Japan). The head of the embryo in the uterus was placed between the tips of a tweezers-type electrode (CUY650-5; Nepa Gene, Chiba, Japan), and electronic pulses (35 V, 50 ms) were discharged five times at intervals of 950 ms with an electroporater (CUY21E; Nepa Gene). The uterine horns were then replaced in the abdominal cavity to allow the embryos to continue normal development.

Time-lapse imaging

Organotypic coronal brain slices (200 μm thick) from the anterior third of the forebrain were prepared using a vibratome (Dosaka, Japan, Kyoto, Japan) at 2 days after electroporation, then placed on a Millicell-CM (pore size, 0.4 μm; Millipore, Bedford, MA, USA), mounted in collagen gel (Nitta Gelatin, Osaka, Japan), and cultured in Neurobasal medium (Gibco BRL, Grand Island, NY, USA) containing 10% fetal calf serum (HyClone, Logan, UT, USA), 0.5 mM L-glutamine and B27 supplement (Invitrogen, San Diego, CA, USA) with or without the NMDA receptor antagonist, 50 μM Cerestat (CNS-1102; Sigma, St Louis, MO, USA) or 10 μM Memantine (Sigma), or α7 nicotinic acetylcholine receptor (nAChR) antagonist, 10 nM methyllycaconitine (MLA, Sigma). The dishes were then mounted in a CO_2 incubator chamber (5% CO_2, at 37 °C) fitted onto a confocal microscope (FV300; Olympus, Tokyo, Japan), and the dorsomedial region of the neocortex was examined. Approximately 10–20 optical Z sections were acquired automatically every 30 min, and ~20 focal planes (~50 μm thick) were merged to visualize the entire shape of the cells.

Tissue preparation and immunohistochemistry

The brain of neonate mouse was dissected out and postfixed in 4% paraformaldehyde (PFA) in PBS for 16 h. After washing in PBS for 1 h, the brain was successively equilibrated in 5%, 10%, and 20% sucrose in PBS, then embedded in optimal cutting temperature compound (Sakura, Tokyo, Japan) and frozen in dry ice. The frozen brain was coronally sectioned at 50 μm with a cryostat (CM-3000; Leica, Nussloch, Germany), and the brain sections were subjected to immunohistochemistry using the floating method. First, the sections were immunostained at 4 °C for 16 h with rabbit polyclonal anti-EGFP antibody (1:500; Invitrogen) in PBS containing 0.1% bovine serum albumin (BSA), 1% normal goat serum, and 0.1% Triton X-100. After successive washes with PBS, the sections were then immunostained at room temperature for 1 h with Alexa Fluor 488 goat anti-rabbit IgG (H+L) (1:1000; Invitrogen) in PBS containing 0.1% BSA, 1% normal goat serum, and 0.1% Triton X-100. In addition, living cultured slices were fixed with 4% PFA at 4 °C for 16 h and subjected to immunohistochemistry using the floating method described above. The slices were immunostained with rat monoclonal anti-nestin antibody (1:500; BD Biosciences, San Jose, CA, USA) coupled to Alexa Fluor 594 goat anti-rat IgG (H+L) (1:1000; Invitrogen) and mounted on silane-coated glass slides with PermaFluor (Thermo Shandon, Pittsburgh, PA, USA). Fluorescence images were obtained with a fluorescence microscope (AX70; Olympus) or a confocal laser microscope (FV1000; Olympus).

Preparation of protein samples from neocortex and immunoblot analysis

At E17.5, pregnant ICR mice were i.p. injected with the NMDA receptor antagonist, Cerestat (5 mg/kg body weight) or Memantine (10 mg/kg body weight; Sigma) or with the same volume of PBS as a control. The mice were then killed 1 h or 1 day after the injection, and the neocortex of the embryos was dissected out and homogenized in lysis buffer (10 mM Tris–HCl [pH 7.4], 150 mM NaCl, 1 mM EDTA, 1% Triton X-100, 0.1% SDS, 0.1% sodium deoxycholate, 1 mM sodium orthovanadate, and a protease inhibitor cocktail [Roche, Mannheim, Germany]) using a Polytron homogenizer. After removing the nuclei and debris by centrifugation (2000×g for 10 min at 4 °C), the protein concentration of the supernatant was determined using BCA Protein Assay Reagent (Pierce, Rockford, IL, USA), and the supernatant was stored at −80 °C until use.

The neocortical proteins were separated by electrophoresis through an SDS polyacrylamide gel (Daiichi, Pure Chemical, Tokyo, Japan) and then electrophoretically transferred to nitrocellulose membranes (Schleicher & Schuell, Dassel, Germany). The membranes were blocked by incubation at room temperature for 1 h with 1% skim milk, 3% skim milk, or 1% BSA in Tris-buffered saline containing 0.1% Tween20 (TBS-T) or StartingBlock T20 Blocking Buffer (Pierce), then incubated at room temperature for 1 h with one of the following primary antibodies in 1% skim milk, 3% skim milk, or 1% BSA in TBS-T or StartingBlock T20 Blocking Buffer: anti-Src-pY418 antibody (1:1000; Biosource International Inc., Camarillo, CA, USA), mouse monoclonal anti-Fyn antibody (1:250, BD Biosciences), mouse monoclonal anti-Yes antibody (1:500, BD Biosciences), mouse monoclonal anti-Src antibody (1:1000; Upstate Biotechnology, Lake Placid, NY, USA), rabbit polyclonal anti-Lyn (H-70) antibody (1:200; Santa Cruz Biotechnology Inc., Santa Cruz, CA, USA), or mouse monoclonal anti-βactin antibody (1:1000; Abcam, Cambridge, UK). After three washes in TBS-T, the membranes were incubated at room temperature for 1 h with horseradish peroxidase-conjugated anti-rabbit IgG secondary antibody (1:1500; Sigma) or horseradish peroxidase-conjugated anti-mouse IgG secondary antibody (1:1500; GE Healthcare, UK Ltd., Buckinghamshire, UK), and washed three times with TBS-T. Immunoreactive bands were visualized using a chemiluminescence detection system (ECL; GE Healthcare, UK Ltd.).

Immunoprecipitation assay

Neocortical proteins (500~1000 μg) were incubated at 4 °C for 2 h with 1 μg of antibody bound to protein A- and G-Sepharose beads (GE Healthcare, UK Ltd). The immunoprecipitates were washed three times with lysis buffer, and after elution by boiling in SDS

sample buffer, the proteins were separated by SDS-polyacrylamide gel electrophoresis (SDS-PAGE) and analyzed by immunoblotting.

Statistical analysis

All the values were expressed as the mean±SEM of n independent observations. Comparisons of multiple groups were performed by using one-way analysis of variance (ANOVA), followed by the Dunnett's test used when two groups were compared. Difference were considered significant when $P<0.05$.

RESULTS

NMDA receptor is involved in the radial migration of immature neurons in the developing mouse neocortex

In a previous BrdU pulse-labeling *in vitro* experiment, we found that the chronic inhibition of NMDA receptors resulted in abnormal neuronal migration and the enhanced proliferation of progenitor cells in developing neocortical slices (Hirasawa et al., 2003). To investigate the role of the NMDA receptor in neocortical development in greater detail, we visualized the newborn neurons using EGFP and examined their migration, including their distribution, morphology, and dynamics, in the present study.

To visualize the newborn neurons in the developing neocortex, we labeled the VZ cells of mouse embryos at E15.5 by transferring the EGFP-encoding plasmid pCAGGS-EGFP using *in utero* electroporation. By placing the anode on the cerebral hemisphere, we could visualize radially migrating neurons derived from the cortical VZ, but not tangentially migrating interneurons originating in ganglionic eminences (Tabata and Nakajima, 2003). We then i.p. injected the pregnant mice with an NMDA receptor antagonist, Cerestat (5 mg/kg body weight) or Memantine (10 mg/kg body weight), or with the same volume of PBS as a control. These injections were performed daily from E17.5 to E19.5. We prepared the brain sections on postnatal day (P) 1 and stained them with anti-EGFP-antibody. In the control sections, more than 60% of the EGFP-positive cells reached the superficial region of the CP. In the sections from the NMDA receptor antagonist-injected mice, however, only about 25% of the EGFP-positive cells reached the superficial region of the CP, but many EGFP-positive cells were seen diffusely scattered throughout the entire CP (Fig. 1A). To perform a quantitative analysis, we divided the CP into five equal bins and counted the number of EGFP-positive cells in each bin and in the intermediate zone (IMZ). As shown in Fig. 1B, the percentage of EGFP-positive cells in each of the bins differed significantly between the sections from the control mice and the NMDA receptor antagonist-injected mice, especially for bin 1 (PBS: 64.6±1.5%, $n=9$ sections; Cerestat: 25.2±0.8%, $n=6$ sections, $P<0.0001$; Memantine: 26.8±1.0%, $n=6$ sections, $P<0.0001$), indicating that the distribution pattern of the EGFP-positive cells in the NMDA receptor antagonist-injected groups was quite different from that in the control group. In contrast, the percentage of EGFP-positive cells in the IMZ of the NMDA receptor antagonist-injected groups significantly increased (PBS: 10.6±0.6%, $n=9$ sections; Cerestat: 20.5±0.8%, $n=6$ sections, $P<0.0001$; Memantine: 24.3±0.9%, $n=6$, $P<0.0001$). Thereafter, at P7, almost all the EGFP-positive cells finally reached the superficial region of the CP and formed the II/III neocortical layer in both NMDA receptor antagonist-injected groups and the control group (Fig. 1C) (bin1; PBS: 90.3±0.4%, $n=6$ sections; Cerestat: 88.5±0.7%, $n=6$ sections; Memantine: 87.3±0.6%, $n=6$ sections). These findings indicate that NMDA receptor is involved in the radial migration of immature neurons and/or the cellular proliferation in the developing neocortex, coincident with a previous BrdU pulse-labeling *in vitro* experiment (Hirasawa et al., 2003).

Migratory profile of the cells in the Cerestat-treated slices differed remarkably from the profile in the control slices

To investigate the dynamics of radially migrating immature neurons, we next performed a time-lapse analysis during NMDA receptor inhibition. We labeled the VZ cells in mouse embryos at E15.5 by transferring pCAGGS-EGFP using *in utero* electroporation; 2 days later, we prepared neocortical slices and cultured them for 24 h in the presence or absence of 50 μM Cerestat. Almost all the EGFP-positive cells in the control slices exhibited a bipolar morphology and moved directly to the CP during radial migration (Fig. 2A–C and Suppl. Movie 1), whereas many EGFP-positive cells in the Cerestat-treated slices dynamically extended and retracted multiple processes, and frequently changed direction (Fig. 2A–C and Suppl. Movie 2). In the Cerestat-treated slices, more than 80% of the EGFP-positive migrating cells exhibited a multipolar shape, while about 20% of the EGFP-positive migrating cells in the control slices exhibited a multipolar morphology (PBS: 21.3±2.1%; Cerestat: 82.5±2.9%, $n=3$). The speed of the cell migration in the Cerestat-treated slices and the control slices was very similar, averaging 11.6±1.3 μm/h in the control slices and 11.7±2.0 μm/h in the Cerestat-treated slices ($n=12$ cells in both slices). These values were consistent with those obtained from the previous studies (9–12 μm/h) (O'Rourke et al., 1992; Tabata and Nakajima, 2003).

To examine whether the aberrant cellular migration caused by Cerestat-treatment is due to the inhibition of NMDA receptor activity, we used Memantine and confirmed that similar results were obtained from slices treated with 10 μM of Memantine (Fig. 3A, B). However, since recent reports have shown that Cerestat and Memantine also affect α7 nAChR (Maskell et al., 2003; Aracava et al., 2005), we investigated the effect of the α7-selective antagonist MLA on neuronal migration. Since previous report showed that 10 nM of MLA completely inhibited the 2 mM acetylcholine-evoked α7 nAChR response in hippocampal slices (Fayuk and Yakel, 2004), we performed the time-lapse analysis in the present of 10 nM MLA. As shown in Fig. 3A, B, there were no significant differences in the neuronal migration including cellular morphology between the control slices and the MLA-treated slices. These results suggest that the aberrant neuronal migration caused by NMDA receptor antagonists is due to the inhibition of NMDA receptor activity.

Since radially migrating cells are thought to be guided by radial glial fibers, we next examined the effect of Cerestat on the formation and arrangement of radial glial fibers

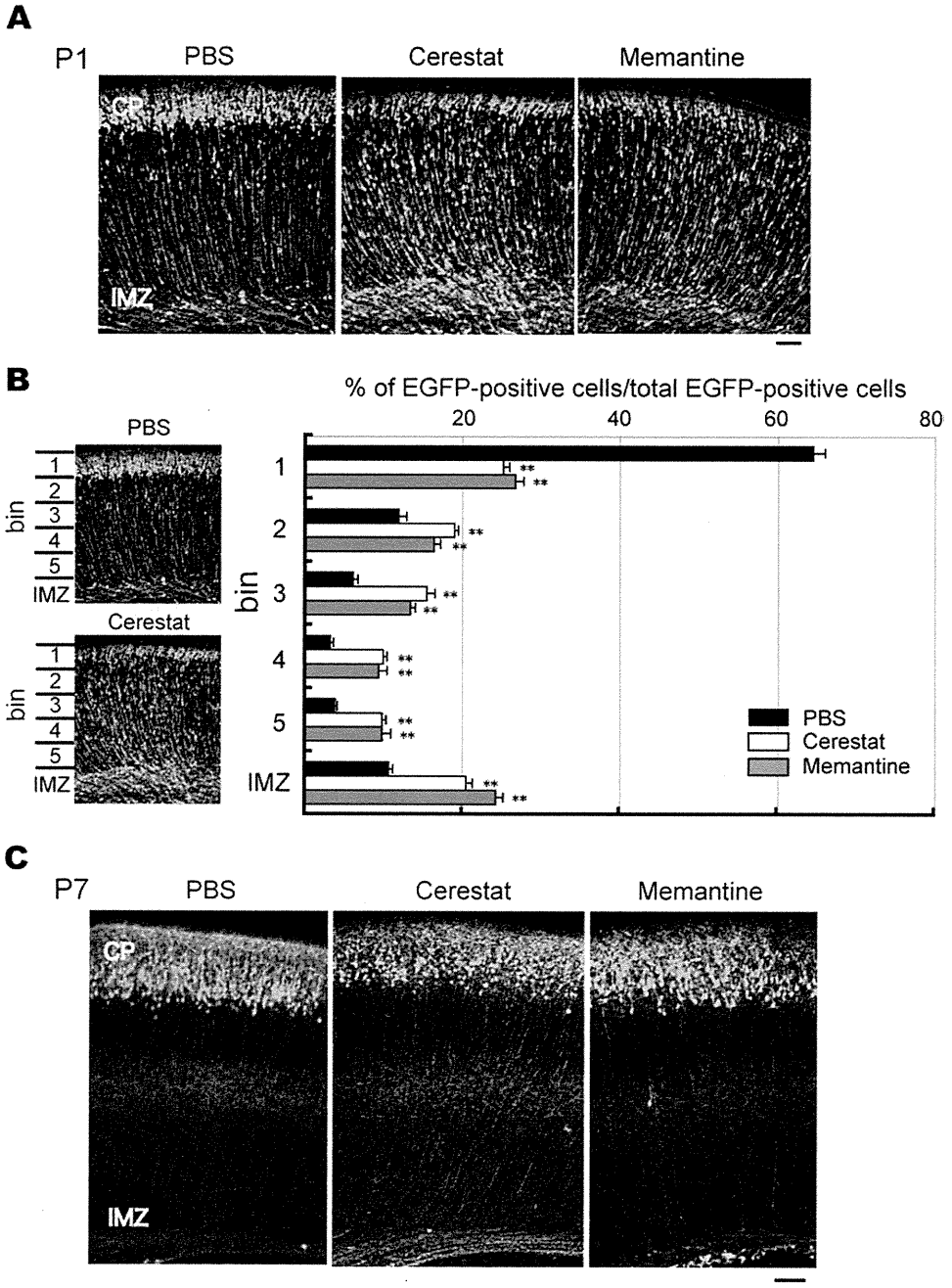

Fig. 1. Localization of EGFP-positive cells in the developing neocortex. (A) Representative images of EGFP-positive cells in neocortical sections of P1 mice. (B) Quantitative analysis of the radial distribution pattern of the EGFP-positive cells in P1 mice. The cortical plate was divided into five equal bins and the number of EGFP-positive cells in the CP and the IMZ was counted. ** $P<0.01$. (C) Representative images of EGFP-positive cells in the neocortical sections of P7 mice. Scale bars=100 μm in panel (A) and 200 μm in panel (C). CP, cortical plate; IMZ, intermediate zone.

by immunostaining with anti-nestin antibody. As shown in Fig. 4A, no apparent differences in the pattern of immunostaining were observed between the slices at either a low or high magnification, indicating that the nestin-positive radial glial fibers aligned normally in the presence of Cerestat. Similar results were obtained from the NMDA receptor antagonist-injected mice (Fig. 4B). These results suggest that the abnormal migration in the Cerestat-treated slices was unlikely related to the radial glial fibers.

Transition from multipolar to bipolar morphology was significantly delayed in migrating cells during NMDA receptor inhibition

Neurons newly generated in the VZ exhibit a multipolar morphology while they remain in the subventricular zone (SVZ) (Tabata and Nakajima, 2003; Noctor et al., 2004) and after a certain period they transform into bipolar cells and migrate into the CP, with a short, thick process extending toward the

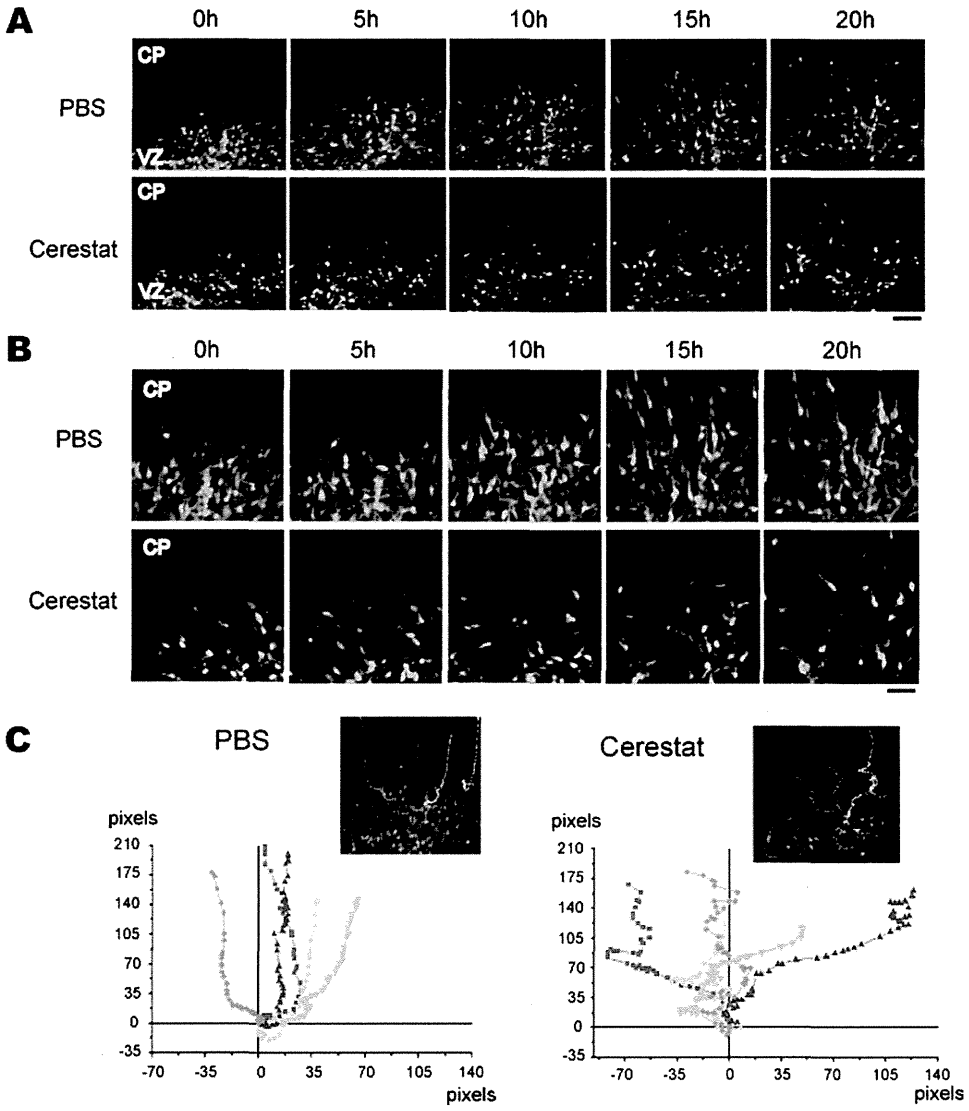

Fig. 2. Analysis of time-lapse images of EGFP-positive migrating cells. (A, B) The movements of EGFP-positive migrating cells were examined in living neocortical slices in the absence (PBS) or presence of 50 μM of Cerestat at a lower (A) and a higher (B) magnification. (C) Tracing of the representative EGFP-positive migrating cells. As shown in the upper panels, which show their initial position, five migrating cells were randomly selected, and their movement was plotted on the graph below. Scale bars=100 μm in panels (A) and 50 μm in panel (B). CP, cortical plate; VZ, ventricular zone.

pial surface (leading process) and an axon-like process extending through the IMZ (Hatanaka et al., 2004). As shown in Fig. 2, time-lapse imaging revealed striking differences in morphology between EGFP-positive migrating cells in the presence of Cerestat and in the control slices. We next investigated the morphological changes and neurite extension that occur during migration. In the control slices, the migrating cells gradually extended their leading process toward the pial surface (Fig. 5A) and properly formed an axon-like process through the IMZ (Fig. 5B) in the Cerestat-treated slices, in contrast, the migrating cells did not form either a leading process or an axon-like process and instead remained multipolar (Fig. 5A, B). These findings suggest that the inhibition of NMDA receptors prevents the morphological change from multipolar to bipolar, and in turn delays neurite extension in the direction of the leading process and axon-like process.

NMDA receptor antagonist down-regulated Src and Fyn activity

To investigate the molecular basis of the NMDA receptor signaling involved in neuronal migration, we focused on Src family kinases (SFKs), since recent studies have shown that SFKs, including Src and Fyn, are important for neuronal migration (Sasaki et al., 2002; Arnaud et al., 2003; Yuasa et al., 2004).

Cerestat was i.p. injected into pregnant mice 1 day or 1 h before the dissection of the neocortex from the embryos at E17.5. The dissected neocortex was homogenized and lysed in lysis buffer. The lysate was centrifuged to remove nuclei and debris, and the concentration of proteins in the supernatant was measured. The results of SDS-PAGE (Fig. 6A) and immunoblotting with anti-β-actin antibody (Fig. 6B) indicated

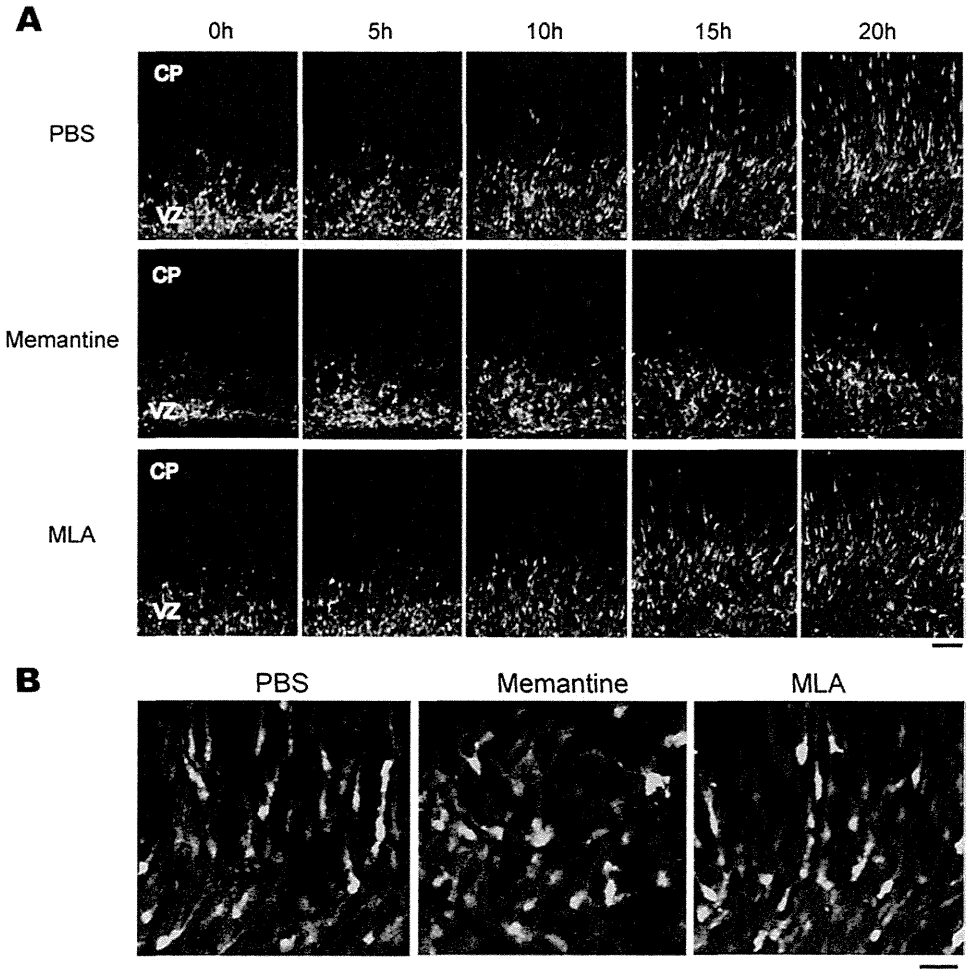

Fig. 3. Analysis of time-lapse images of EGFP-positive migrating cells. (A) The movements of EGFP-positive migrating cells were examined in living neocortical slices in the absence (PBS) or presence of 10 μM of Memantine or 10 nM of methyllycaconitine (MLA). (B) Representative images of EGFP-positive cells at 20 h. The cells are moving toward the upper side. Scale bars=100 μm in panels (A) and 50 μm in panel (B). CP, cortical plate; VZ, ventricular zone.

that the protein concentrations of the samples were almost equal. The immunoblot analysis (Fig. 6B) and quantitative analysis (Fig. 6D) were performed with anti-Src pY418 antibody, which detects an activated form of SFKs (Thomas and Brugge, 1997), and showed that Cerestat had caused a significant decrease in the activated form of SFKs (1 h: 0.41 ± 0.05, $n=3$, $P<0.01$; 1 day: 0.79 ± 0.06, $n=3$, $P<0.01$), suggesting that Cerestat had suppressed SFKs activity. Similar results were obtained from the protein samples treated with Memantine (Fig. 6C) (0.34 ± 0.04, $n=3$, $P<0.01$). These results suggest that NMDA receptors are involved in the regulation of SFKs activity in the developing neocortex.

The catalytic SH2 domain recognized by anti-Src pY418 antibody is highly conserved among SFKs; as a result, this antibody also reacts with Fyn, Yes, and Lyn, all of which are expressed in neocortical neurons. We then performed an immunoprecipitation assay to identify the kinase involved in NMDA receptor signaling. We first confirmed that the levels of expression of Src, Fyn, Yes, and Lyn in the Cerestat-exposed sample and the control sample were very similar (Fig. 7A). In the control sample, the anti-Src pY418 antibody precipitated Src and Fyn, but not Yes or Lyn. The signals detected by anti-Src and anti-Fyn antibodies decreased in the Cerestat-exposed sample (Fig. 7B). In contrast, in the precipitates obtained with the anti-Src and anti-Fyn antibodies, a lower level of the activated form of kinase detected by anti-Src pY418 antibody was found in the Cerestat-exposed sample (Fig. 7C). These results indicate that the inhibition of NMDA receptors caused the decrease in Src and Fyn activity. On the other hand, anti-Lyn antibody precipitated Lyn and anti-Yes antibody precipitated Yes (Fig. 7D), but the signals detected by anti-Src pY418 in the precipitates were faint, with similar levels observed in the Cerestat-exposed sample and the control sample (Fig. 7C), suggesting that Lyn and Yes are not involved in NMDA receptor signaling.

DISCUSSION

To investigate the role of the NMDA receptor in neocortical development, we visualized the immature neurons by transferring the EGFP-encoding plasmid pCAGGS-EGFP into the VZ cells of mouse neocortex at E15.5 using *in*

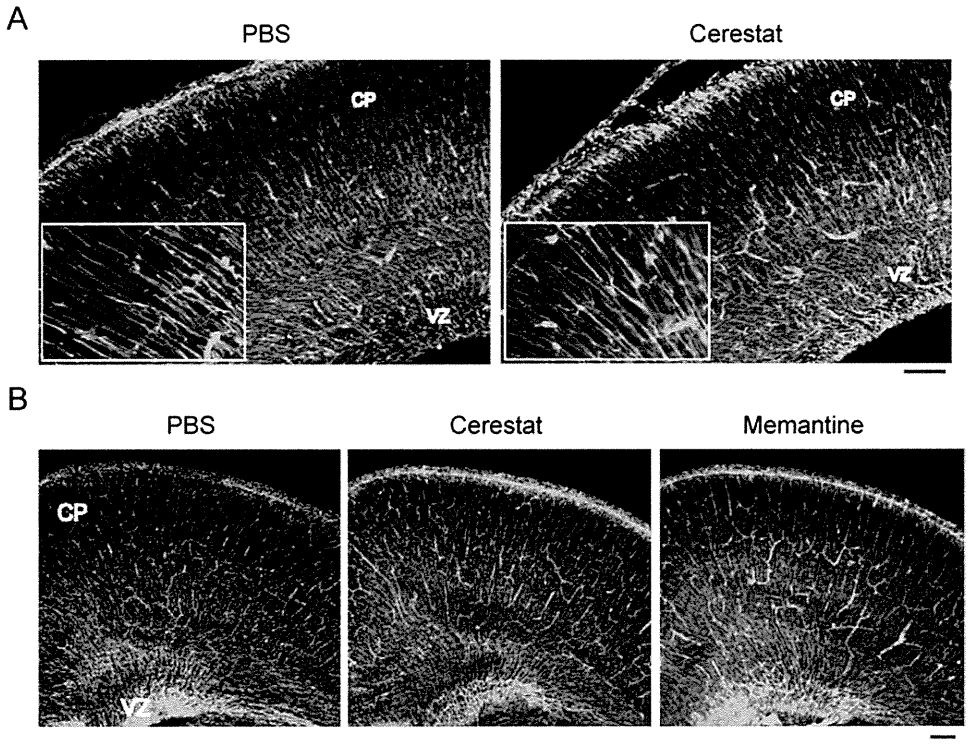

Fig. 4. Representative images of immunostaining with anti-nestin antibody. (A) The neocortical slices were prepared from mouse embryos at E17.5. After 24 h cultivation in the absence (PBS) or presence of 50 μM Cerestat, they were immunostained with anti-nestin antibody. The inset shows confocal microphotographs at a higher magnification. (B) Pregnant mice were injected with PBS, Cerestat or Memantine daily from E17.5 to E19.5. The neocortical sections were prepared on P1 and immunostained with anti-nestin antibody. Scale bars=100 μm. CP, cortical plate; VZ, ventricular zone.

utero electroporation. At P1, as shown in Fig. 1, the EGFP-positive cells in the NMDA antagonist-injected mice were distributed throughout the entire CP. One possible explanation for this observation is a defect in cellular migration

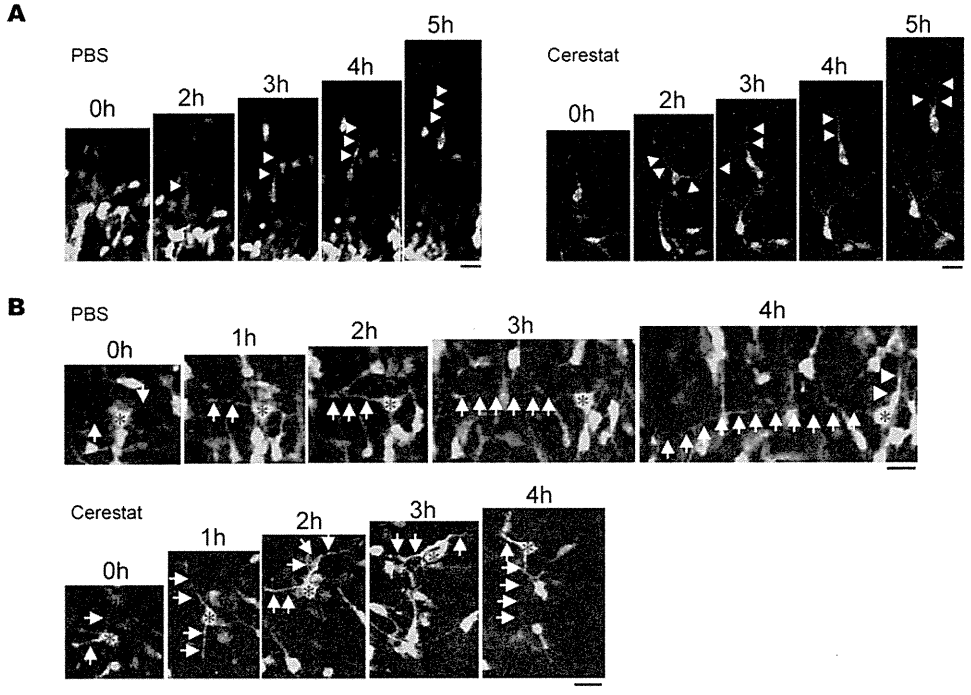

Fig. 5. Morphological changes in the EGFP-positive migrating cells. Time-lapse images of the formation of the leading process (arrowheads in A) and the axon-like process (arrows in B). Scale bars=20 μm.

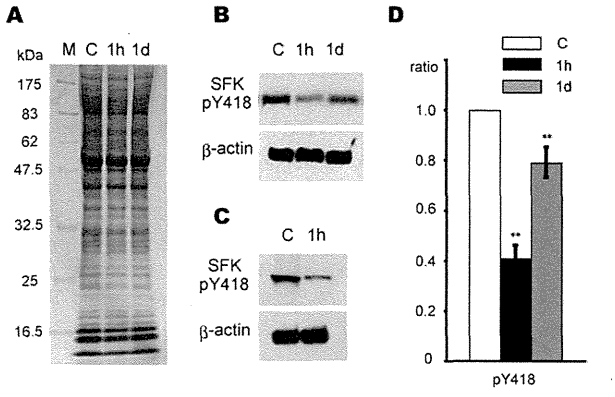

Fig. 6. NMDA receptors regulate the activity of SFKs in the developing neocortex. (A) SDS-PAGE analysis. At E17.5 pregnant mice were injected with Cerestat or the same volume of PBS as a control (lane C). The neocortex of the embryos was dissected out 1 h (lane 1h) or 1 d (lane 1d) later and used to prepare neocortical protein samples. The protein samples (30 μg) were subjected to SDS-PAGE and subsequent staining with Coomassie Blue. Molecular weight standards are shown on the left. (B, C) Immunoblot analysis of protein samples prepared from embryos of a pregnant mouse injected with Cerestat (B) or Memantine (C). The protein samples (15 μg of protein for Src pY418 and 20 μg of protein for β-actin) were subjected to an immunoblot analysis using the indicated antibodies. (D) A quantitative analysis of the immunoblot shown in Fig. 4B. The relative strength of the band signals was measured using NIH Imaging software, and the ratios were calculated by dividing the value of each sample by the value of the control sample. ** $P<0.01$.

caused by the NMDA receptor antagonist. However, many EGFP-positive cells were observed in the IMZ (below bin 5) in the NMDA antagonist-injected group. Since our previous report showed that an NMDA receptor antagonist increased the proliferation of progenitor cells in the VZ (Hirasawa et al., 2003), more EGFP-positive cells were likely born in the VZ of the NMDA receptor antagonist-injected mice even after E17, resulting in the numerous EGFP-positive cells observed in the IMZ. Therefore, the difference in the distribution pattern of the EGFP-positive cells might have been caused not only by a defect of neuronal migration, but also by an NMDA receptor antagonist-induced enhancement of cellular proliferation.

It is difficult to confirm whether a drug treated i.p. via the mother is directly effective for the embryos. Therefore, to investigate directly the dynamics of radial migration under the inhibition of NMDA receptor activity, we next performed a time-lapse analysis of living neocortical slices prepared from E17.5 mouse embryos. Recent studies have shown that at E17.5 newborn neurons derived from the VZ at E15.5 are located in the VZ-IMZ and that these cells reach the CP on the following day (E18.5) (Tabata and Nakajima, 2003; Noctor et al., 2004; Hatanaka et al., 2004). These immature neurons undergo changes in orientation and morphology as they migrate, and the immature neurons that reach the IMZ-CP border are oriented toward the pial surface. Once integrated into the CP, they exhibit a typical bipolar morphology, with a leading process extending toward the pial surface and an axon-like process extending through the IMZ (both of which are closely apposed to radial glial fibers), and the cells proceed directly to their final destination. This migratory behavior is referred to as "locomotion", and this movement probably corresponds to glial cell-guided migration (Nadarajah et al., 2001). The analysis of time-lapse images in this study revealed that many migrating cells that had been exposed to an NMDA receptor antagonist exhibited a multipolar morphology and repeatedly extended and retracted their processes in a very dynamic manner. Moreover, instead of migrating straight toward the pial surface, they frequently changed direction, although ultimately they generally tended to move toward the pial surface. Thus, the migratory mode during NMDA receptor inhibition was quite different from the mode observed in the control slices. Multipolar migration resembling the migratory mode observed during NMDA receptor inhibition was recently observed in living neocortical slices prepared from E14 mouse embryos (Tabata and Nakajima, 2003). However, such movement was only observed in the SVZ/IMZ, not in the CP, and the rate of multipolar migration was much slower (4.4 μm/h) than that of the migrating cells observed during NMDA receptor inhibition (11.7 μm/h), which was comparable to the rate observed in the control slices in the present study (11.6 μm/h) and previous reports (9–12

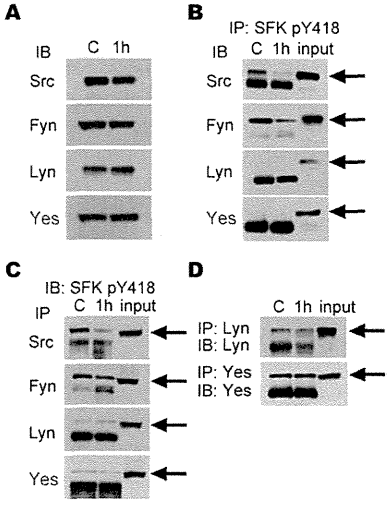

Fig. 7. Activation of Src and Fyn in the developing neocortex is regulated by NMDA receptors. (A) Immunoblot analysis. At E17.5, pregnant mice were injected with Cerestat or the same volume of PBS as a control (lane C). The neocortex of the embryos was dissected out 1 h (lane 1h) later and used to prepare neocortical protein samples. The protein samples (10 μg of protein for Src; 15 μg of protein for Fyn, Lyn and Yes) were subjected to an immunoblot analysis using the indicated antibodies. (B) Immunoprecipitation assay. Anti-Src pY418 antibody bound to Protein A- and G-Sepharose beads was incubated with the protein samples (600 μg of protein for Src and Fyn; 1 mg of protein for Lyn and Yes). After washing, the proteins on the beads were eluted with SDS-PAGE sample buffer and immunoblotted with the indicated antibodies. (C) Immunoprecipitation assay. The indicated antibody bound to Protein A- and G-Sepharose beads was incubated with the protein samples (600 μg of protein for Src and Fyn; 1 mg of protein for Lyn and Yes). After washing, the proteins on the beads were eluted with SDS-PAGE sample buffer and immunoblotted with anti-Src pY418 antibody. (D) Immunoprecipitation assay. Anti-Lyn or anti-Yes antibody bound to Protein A- and G-Sepharose beads was incubated with the protein samples (1 mg). After washing, the proteins on the beads were eluted with SDS-PAGE sample buffer and immunoblotted with anti-Lyn or anti-Yes antibody. The signals are indicated by the arrows.

μm/h) (O'Rourke et al., 1992; Tabata and Nakajima, 2003). Therefore, the migratory mode during NMDA receptor inhibition might differ from the multipolar migration observed in the normal developing neocortex.

In this study, we observed that NMDA receptor antagonist suppressed Src and Fyn activities. Recent cumulative evidence has shown that SFKs, including Src and Fyn, play an important role in neuronal migration. Yuasa et al. (2004) reported that Fyn was intensely expressed in migratory neurons of the IMZ, with most of the Fyn localized in the leading process that elongated radially in the migratory direction; furthermore, neocortical neurons labeled with BrdU at E16 in Fyn-deficient mice were aberrantly distributed. These results were very similar to our results, shown in Fig. 1, and those obtained in our previous study (Hirasawa et al., 2003). Furthermore, Reelin is well known as an important molecule in the control of cell migration and the positioning of immature neurons in the developing neocortex. Recent studies have shown that the tyrosine phosphorylation of Disabled-1 (Dab-1) by Src and Fyn is a key event in Reelin signaling (Howell et al., 2000; Keshvara et al., 2001; Arnaud et al., 2003; Bock and Herz, 2003; Kuo et al., 2005). In addition, focal adhesion kinase (FAK) has also been found to be involved in neuronal migration in the developing neocortex, including neurite extension and the guidance of growth cone turning (Girault et al., 1999; Beggs et al., 2003; Rico et al., 2004). FAK is phosphorylated in response to a variety of stimuli (Schaller et al., 1994; Calalb et al., 1995; Girault et al., 1999), and FAK phosphorylation is critical to the regulation of downstream signaling molecules, including PLC-γ, PI3K, Akt and Rac (Kornberg et al., 1991; Guan and Shalloway, 1992; Schaller et al., 1992; Girault et al., 1999; Parsons, 2003). Interestingly, we found that an NMDA receptor antagonist dramatically reduced the Y861 phosphorylation of FAK (unpublished data), which is regulated by SFKs. Recent studies have shown that FAK is a downstream mediator in the netrin signaling pathway (Li et al., 2004; Liu et al., 2004). Netrins have various neuronal functions in the developing brain, including the promotion of axonal outgrowth, the guidance of growth cone turning, and the regulation of neuronal branching (Culotti and Merz, 1998; Livesey, 1999). Using *Xenopus laevis* spinal neurons Ren et al. (2004) clearly demonstrated that Y861 phosphorylation is critical for netrin-1 induced growth cone turning responses. Furthermore, Zheng et al. (1996) found that APV, an NMDA receptor antagonist, blocked the turning response of the growth cone in *Xenopus* spinal neurons. These results suggest that NMDA receptor antagonist-induced suppression of Y861 phosphorylation causes a defect in the morphological maturation of immature neurons.

Src and Fyn are important to neuronal migration in the developing neocortex. The present results suggest that the NMDA receptor-mediated activation of Src and Fyn is a critical event in the morphological conversion of immature neurons from multipolar cells to bipolar cells that migrate radially towards the pial surface. SFKs, including Src and Fyn, are widely known to phosphorylate NMDA receptors and to regulate their activities (Tezuka et al., 1999; Nakazawa et al., 2001). On the other hand, Metere et al. (2006) reported that quinolic acid, an NMDA receptor agonist, increases Src activity. Thus, a complex and mutually regulatory interaction likely exists between NMDA receptors and SFKs. Further study is needed to elucidate the molecular basis of the NMDA receptor signaling pathway in neuronal migration.

Acknowledgments—We thank Drs. Shigeki Yuasa and Kotaro Hattori for useful advice. This study was supported by grants from the Ministry of Health, Labour and Welfare of Japan, and from the Ministry of Education, Culture, Sports and Science and Technology of Japan.

REFERENCES

Angevine JB, Sidman RL (1961) Autoradiographic study of cell migration during histogenesis of cerebral cortex in the mouse. Nature 192:766–768.

Aracava Y, Pereira EFR, Maelicke A, Albuquerque EX (2005) Memantine blocks α7 nicotinic acetylcholine receptor more potently than *N*-methyl-D-aspartate receptors in rat hippocampal neurons. J Pharmacol Exp Ther 312:1195–1205.

Arnaud L, Ballif BA, Forster E, Cooper JA (2003) Fyn tyrosine kinase is a critical regulator of Disabled-1 during brain development. Curr Biol 13:9–17.

Beggs HE, Schahin-Reed D, Zang K, Goebbels S, Nave K-A, Gorski J, Jones KR, Sretavan D, Reichardt LF (2003) FAK deficiency in cells contributing to the basal lamina results in cortical abnormalities resembling congenital muscular dystrophies. Neuron 40:501–514.

Behar TN, Scott CA, Greene CL, Wen X, Smith SV, Maric D, Liu QY, Colton CA, Barker JL (1999) Glutamate acting at NMDA receptors stimulates embryonic cortical neuronal migration. J Neurosci 19:4449–4461.

Berry M, Rogers AW (1965) The migration of neuroblasts in the developing cerebral cortex. J Anat 99:691–709.

Bock HH, Herz J (2003) Reelin activates SRC family tyrosine kinases in neurons. Curr Biol 13:18–26.

Calalb MB, Polte TR, Hanks SK (1995) Tyrosine phosphorylation of focal adhesion kinase at sites in the catalytic domain regulates kinase activity: a role for Src family kinases. Mol Cell Biol 15:954–963.

Culotti JG, Merz DC (1998) DCC and netrins. Curr Opin Cell Biol 10:609–613.

Fayuk D, Yakel JL (2004) Regulation of nicotinic acetylcholine receptor channel function by acetylcholinesterase inhibitors in rat hippocampal CA1 interneurons. Mol Pharmacol 66:658–666.

Girault JA, Costa A, Derkinderen P, Studler JM, Toutant M (1999) FAK and PYK/CAKβ in the nervous system: a link between neuronal activity, plasticity and survival? Trends Neurosci 22:257–263.

Guan JL, Shalloway D (1992) Regulation of focal adhesion-associated protein tyrosine kinase by both cellular adhesion and oncogenic transformation. Nature 358:690–692.

Hatanaka Y, Hisanaga S, Heizmann CW, Murakami F (2004) Distinct migratory behavior of early- and late-born neurons derived from the cortical ventricular zone. J Comp Neurol 479:1–14.

Heng JI, Moonen G, Nguyen L (2007) Neurotransmitters regulate cell migration in the telencephalon. Eur J Neurosci 26:537–546.

Hirai K, Yoshioka H, Kihara M, Hasegawa K, Sakamoto T, Sawada T, Fushiki S (1999) Inhibiting neuronal migration by blocking NMDA receptors in the embryonic rat cerebral cortex: a tissue culture study. Brain Res Dev Brain Res 114:63–67.

Hirasawa T, Wada H, Kohsaka S, Uchino S (2003) Inhibition of NMDA receptors induces delayed neuronal maturation and sustained proliferation of progenitor cells during neocortical development. J Neurosci Res 74:676–687.

Howell BW, Herrick TM, Hildebrand JD, Zhang Y, Cooper JA (2000) Dab1 tyrosine phosphorylation sites relay positional signals during mouse brain development. Curr Biol 10:877–885.

Keshvara L, Benhayon D, Magdaleno S, Curran T (2001) Identification of reelin-induced sites of tyrosyl phosphorylation on disabled. 1. J Biol Chem 276:16008–16014.

Kihara M, Yoshioka H, Hirai K, Hasegawa K, Kizaki Z, Sawada T (2002) Stimulation of *N*-methyl-D-aspartate (NMDA) receptors inhibits neuronal migration in embryonic cerebral cortex: a tissue culture study. Brain Res Dev Brain Res 138:195–198.

Komuro H, Rakic P (1993) Modulation of neuronal migration by NMDA receptors. Science 260:95–97.

Kornberg L, Earp SE, Turner CE, Procktop C, Juliano RL (1991) Signal transduction by integrins: increased protein tyrosine phosphorylation caused by clustering of b1 integrins. Proc Natl Acad Sci U S A 88:8392–8396.

Kuo G, Arnaud L, Kronstad-O'Brien P, Cooper JA (2005) Absence of Fyn and Src causes a reeler-like phenotype. J Neurosci 25: 8578–8586.

Li W, Lee J, Vikis HG, Lee S-H, Liu G, Aurandt J, Shen T-L, Fearon ER, Guan J-L, Han M, Rao Y, Hong K, Guan K-L (2004) Activation of FAK and Src are receptor-proximal events required for netrin signaling. Nat Neurosci 7:1213–1221.

Liu G, Beggs H, Jürgensen C, Park H-T, Tang H, Gorski J, Jones KR, Reichardt LF, Wu J, Rao Y (2004) Netrin requires focal adhesion kinase and Src family kinases for axon outgrowth and attraction. Nat Neurosci 7:1222–1232.

Livesey FJ (1999) Netrins and netrin receptors. Cell Mol Life Sci 56:62–68.

Luján R, Shigemoto R, López-Bendito G (2005) Glutamate and GABA receptor signaling in the developing brain. Neuroscience 130: 567–580.

Manent J-B, Demarque M, Jorquera I, Pellegrino C, Ben-Ari Y, Aniksztejn L, Represa A (2005) A noncanonical release of GABA and glutamate modulates neuronal migration. J Neurosci 25:755–4765.

Marin O, Rubenstein JL (2001) A long, remarkable journey: tangential migration in the telencephalon. Nat Rev Neurosci 2:780–790.

Maskell PD, Speder P, Newberry NR, Bermudez I (2003) Inhibition of human $\alpha 7$ nicotinic acetylcholine receptors by open channel blockers of *N*-methyl-D-aspartate receptors. Br J Pharmacol 140:1313–1319.

Metere A, Mallozzi C, Minetti M, Domenici MR, Pézzola A, Popoli P, Di Stasi AM (2006) Quinolinic acid modulates the activity of *src* family kinases in rat striatum: *in vivo* and *in vitro* studies. J Neurochem 97:1327–1336.

Nadarajah B, Brunstrom JE, Grutzendler J, Wong RO, Pearlman AL (2001) Two mode of radial migration in early development of the cerebral cortex. Nat Neurosci 4:143–150.

Nakahira E, Yuasa S (2005) Neuronal generation, migration, and differentiation in the mouse hippocampal primordium as revealed by enhanced green fluorescent protein gene transfer by means of *in utero* electroporation. J Comp Neurol 483:329–340.

Nakajima K (2007) Control of tangential/non-radial migration of neurons in the developing cerebral cortex. Neurochem Int 51:121–131.

Nakazawa T, Komai S, Tezuka T, Hisatsune C, Umemori H, Semba K, Mishina M, Manabe T, Yamamoto T (2001) Characterization of Fyn-mediated tyrosine phosphorylation sites on GluR $\varepsilon 2$ (NR2B) subunit of the N-methyl-D-aspartate receptor. J Biol Chem 276: 693–699.

Noctor SC, Martínez-Cerdeno V, Ivic L, Kringstein AR (2004) Cortical neurons arise in symmetric and asymmetric division zones and migrate through specific phases. Nat Neurosci 7:136–144.

O'Rourke NA, Dailey ME, Smith SJ, McConnell SK (1992) Diverse migratory pathways in the developing cerebral cortex. Science 258:299–302.

Parsons JT (2003) Focal adhesion kinase: the first ten years. J Cell Sci 116:1409–1416.

Rakic P (1972) Mode of cell migration to the superficial layers of fetal monkey neocortex. J Comp Neurol 145:61–84.

Ren X, Ming G, Xie Y, Hong Y, Sun D, Zhao Z, Feng Z, Wang Q, Shim S, Chen Z, Song H, Mei L, Xiong W (2004) Focal adhesion kinase in netrion-1 signaling. Nat Neurosci 7:1204–1212.

Rico B, Beggs HE, Schahin-Reed D, Kimes N, Schmidt A, Reichardt LF (2004) Control of axonal branching and synapse formation by focal adhesion kinse. Nat Neurosci 7:1059–1069.

Sasaki Y, Cheng C, Uchida Y, Nakajima O, Ohshima T, Yagi T, Taniguchi M, Nakayama T, Kishida R, Kudo Y, Ohno S, Nakamura F, Goshima Y (2002) Fyn and Cdk5 mediate semaphorin-3A signaling, which is involved in regulation of dendrite orientation in cerebral cortex. Neuron 35:907–920.

Schaller MD, Borgman CA, Cobb BS, Reynolds AB, Parsons JT (1992) pp125FAK, a structurally distinctive protein tyrosine kinase associated with focal adhesions. Proc Natl Acad Sci U S A 89:5192–5196.

Schaller MD, Hildebrand JD, Shannon JD, Fox JW, Vines RR, Parsons JT (1994) Autophosphorylation of the focal adhesion kinse, pp125FAK, directs SH2-dependent binding of pp60src. Mol Cell Biol 14:1680–1688.

Simonian SX, Herbison AE (2001) Differing, spatially restricted roles of ionotropic glutamate receptors in regulating the migration of GnRH neurons during embryogenesis. J Neurosci 21:934–943.

Tabata H, Nakajima K (2001) Efficient *in utero* gene transfer system to the developing mouse brain using electroporation: visualization of neuronal migration in the developing cortex. Neuroscience 103:865–872.

Tabata H, Nakajima K (2003) Multipolar migration: the third mode of radial neuronal migration in the developing cerebral cortex. J Neurosci 23:9996–10001.

Tezuka T, Umemori H, Akiyama T, Nakanishi S, Yamamoto T (1999) PSD-95 promotes Fyn-mediated tyrosine phosphorylation of the N-methyl-D-aspartate receptor subunit NR2A. Proc Natl Acad Sci U S A 96:435–440.

Thomas SM, Brugge JS (1997) Cellular functions regulated by Src family kinases. Annu Rev. Cell Dev Biol 13:513–609.

Yozu M, Tabata H, Konig N, Nakajima K (2008) Migratory behavior of presumptive interneurons is affected by AMPA receptor activation in slice cultures of embryonic mouse neocortex. Dev Neurosci 30:105–116.

Yuasa S, Hattori K, Yagi T (2004) Defective neocortical development in Fyn-tyrosine-kinase-deficient mice. Neuroreport 15:819–822.

Zheng JQ, Wan J, Poo M (1996) Essential role of filopodia in chemotropic turning of nerve growth cone induced by a glutamate gradient. J Neurosci 16:1140–1149.

APPENDIX

Supplementary data

Supplementary data associated with this article can be found, in the online version, at doi:10.1016/j.neuroscience.2010.05.024.

(Accepted 12 May 2010)
(Available online 16 May 2010)

Neuroscience 167 (2010) 372–383

PIGMENT EPITHELIUM-DERIVED FACTOR UP-REGULATION INDUCED BY MEMANTINE, AN N-METHYL-D-ASPARTATE RECEPTOR ANTAGONIST, IS INVOLVED IN INCREASED PROLIFERATION OF HIPPOCAMPAL PROGENITOR CELLS

T. NAMBA,[a1] T. YABE,[b] Y. GONDA,[a] N. ICHIKAWA,[c] T. SANAGI,[a] E. ARIKAWA-HIRASAWA,[c] H. MOCHIZUKI,[d] S. KOHSAKA[a]* AND S. UCHINO[a]

[a]*Department of Neurochemistry, National Institute of Neuroscience, Tokyo 187-8502, Japan*

[b]*Kitasato Institute for Life Sciences, Kitasato University, Tokyo 108-8641, Japan*

[c]*Research Institute for Diseases of Old Age, Juntendo University School of Medicine, Tokyo 113-8431, Japan*

[d]*Department of Neurology, Kitasato University, Kanagawa 228-8555, Japan*

Abstract—Memantine is classified as an NMDA receptor antagonist. We recently reported that memantine promoted the proliferation of neural progenitor cells and the production of mature granule neurons in the adult hippocampus. However, the molecular mechanism responsible for the memantine-induced promotion of cellular proliferation remains unknown. In this study we searched for a factor that mediates memantine-induced cellular proliferation, and found that pigment epithelium-derived factor (PEDF), a broad-acting neurotrophic factor, is up-regulated in the dentate gyrus of adult mice after the injection of memantine. PEDF mRNA expression increased significantly by 3.5-fold at 1 day after the injection of memantine. In addition, the expression level of PEDF protein also increased by 1.8-fold at 2 days after the injection of memantine. Immunohistochemical study using anti-PEDF antibody showed that the majority of the PEDF-expressing cells were protoplasmic and perivascular astrocytes. Using a neurosphere assay, we confirmed that PEDF enhanced cellular proliferation under the presence of fibroblast growth factor-2 (FGF-2) and epidermal growth factor (EGF) but was not involved in the multilineage potency of hippocampal progenitor cells. Over expression of PEDF by adeno-associated virus, however, did not stimulate cellular proliferation, suggesting PEDF *per se* does not promote cellular proliferation *in vivo*. These findings suggest that the memantine induced PEDF up-regulation is involved in increased proliferation of hippocampal progenitor cells.

Key words: neurogenesis, hippocampus, PEDF, NMDA receptor, memantine.

Neurogenesis persists throughout life in the hippocampi of mammals, including humans (Altman and Das, 1965; Seki and Arai, 1993; Eriksson et al., 1998; Ming and Song, 2005; Namba et al., 2005). Neural progenitor cells divide and give rise to new neurons in at least two regions of the adult brain: the dentate gyrus (DG) of the hippocampus and the subventricular zone (SVZ) of the lateral ventricle (Alvarez-Buylla et al., 2002; Ming and Song, 2005). We recently demonstrated that memantine, an uncompetitive N-methyl-D-aspartate (NMDA) receptor antagonist that is used clinically for the treatment of Alzheimer's disease, increased the proliferation of progenitor cells and promoted the subsequent production of new neurons in adult hippocampus (Maekawa et al., 2009; Namba et al., 2009). However, the molecular mechanism responsible for the memantine-induced promotion of cellular proliferation remains unclear. Since recent electrophysiological studies have shown that progenitor cells in adult hippocampus fail to respond to NMDA (Tozuka et al., 2005), functional NMDA receptors are probably not expressed in progenitor cells (Petrus et al., 2009). Therefore, indirect mechanisms might underlie the effect of memantine on the proliferation of progenitor cells. Previous studies have demonstrated that brain-derived neurotrophic factor (BDNF) and fibroblast growth factor-2 (FGF-2) are up-regulated by treatment with memantine (Marvanova et al., 2001; Namba et al., 2009). However, no evidence suggesting that BDNF and FGF-2 stimulate the proliferation of hippocampal progenitor cells has been obtained (Kuhn et al., 1997; Wagner et al., 1999; Sairanen et al., 2005), although BDNF has been shown to influence the survival of newly generated cells (Sairanen et al., 2005). In the present study, we found that pigment epithelium-derived factor (PEDF), in addition to BDNF and FGF-2, was up-regulated by treatment with memantine.

PEDF is a 50-kDa glycoprotein and a non-inhibitory member of the serine protease inhibitor gene family (Tombran-Tink and Barnstable, 2003). Its biological activity was first identified in a conditioned medium of cultured human fetal retinal pigment epithelial cells, which induced the neuronal differentiation of cultured human Y-79 retinoblastoma cells (Tombran-Tink et al., 1991). PEDF is expressed in various regions of the brain, including neuronal and glial cells, and has neurotrophic and neuroprotective effects in

[1] Present address: Department of Cell Pharmacology, Nagoya University Graduate School of Medicine, Nagoya 466-8550, Japan.

*Corresponding author. Tel: +81-42-346-1711; fax: +81-42-346-1741.
E-mail address: kohsaka@ncnp.go.jp (S. Kohsaka).

Abbreviations: AAV, adeno-associated virus; AD, Alzheimer's disease; BDNF, brain-derived neurotrophic factor; BrdU, 5-bromo-2-deoxyuridine; BSA, bovine serum albumin; DG, dentate gyrus; FGF-2, fibroblast growth factor-2; GAPDH, glyceraldehydes-3-phosphate dehydrogenase; GCL, granule cell layer; GFAP, glial fibrillary acidic protein; NMDA, N-methyl-D-aspartate; PEDF, pigment epithelium-derived factor; PFA, paraformaldehyde; RT-PCR, reverse transcription-PCR; SVZ, subventricular zone.

0306-4522/10 $ - see front matter © 2010 IBRO. Published by Elsevier Ltd. All rights reserved.
doi:10.1016/j.neuroscience.2010.01.033

various types of neurons (Tombran-Tink and Barnstable, 2003; Yabe et al., 2005; Sanagi et al., 2007). Interestingly, Ramirez-Castillejo et al. (2006) showed that PEDF was secreted from ependymal and endothelial cells of adult SVZ and promoted the self-renewal of adult neural stem cells in the SVZ; these results indicated that PEDF plays a role in the maintenance of neural stem cells, functioning as a niche-derived regulator in the SVZ (Ramirez-Castillejo et al., 2006). In the present study, we provide novel findings showing that the expression of PEDF was increased by treatment with memantine and that PEDF promoted the proliferation of hippocampal progenitor cells, suggesting that PEDF is an intriguing factor involved in the memantine-induced promotion of cellular proliferation in adult hippocampus.

EXPERIMENTAL PROCEDURES

The animals used in this study were 3-month-old male and postnatal day 1 (P1) C57BL6/J mice (Clea Japan Inc., Tokyo, Japan). All experimental procedures were approved by The Animal Care and Use Committee of the National Institute of Neuroscience.

Animals and drug administration

Mice were injected i.p. with memantine (Sigma, St. Louis, MO, USA) at a dose of 10, 30, or 50 mg/kg body weight. Control mice were injected i.p. with the same volume of 0.9% saline (Ohtsuka Pharmaceuticals, Tokyo, Japan). After 1, 2, or 3 days, the mice were injected i.p. with 75 mg/kg body weight of 5-bromo-2-deoxyuridine (BrdU; Sigma) three times at intervals of 2 h. The mice were then sacrificed at 1 day after BrdU-injection.

Tissue preparation

After the mice were deeply anesthetized with sodium pentobarbital (Kyoritsu Pharmaceuticals, Tokyo, Japan), the mice were transcardially perfused with 4% paraformaldehyde (PFA) in 0.1 M phosphate-buffered saline (PBS). The brains were then removed and immersion-fixed at 4 °C overnight in the same fixative. After washing in PBS, the brains were successively equilibrated in 10 and 20% sucrose in PBS, embedded in Tissue-Tek optimal cutting temperature compound (Sakura, Tokyo, Japan), and frozen in liquid nitrogen (Seki et al., 2007).

Immunohistochemistry

For immunostaining with anti-BrdU antibody, frozen brains were coronally sliced into 14-μm sections using a cryostat (CM-3000; Leica, Nussloch, Germany) and mounted on an MAS-coated glass slide (SUPERFROST; Matsunami, Osaka). The sections were boiled in 0.01 M citrate buffer for 15 min, incubated in 2N HCl at 37 °C for 35 min, and washed in PBS. The sections were then incubated with rat monoclonal anti-BrdU antibody (1:400; Morpho-Sys UK Ltd., Oxford, UK) at 4 °C overnight in PBS containing 1% bovine serum albumin (BSA). After washing in PBS, they were then incubated at room temperature for 1–2 h in PBS containing 1% BSA plus Cy3-conjugated anti-rat IgG antibody (1:200; Jackson, West Grove, PA, USA). For immunostaining with other antibodies, immunohistochemistry was performed using a floating method as described previously (Namba et al., 2009). Briefly, the frozen brains were coronally sliced into 40-μm sections using a cryostat (CM-3000). After washing in PBS, the sections were incubated at 4 °C overnight with rabbit polyclonal anti-PEDF antibody (1:400; Sanagi et al. (2007)) and mouse monoclonal anti-glial fibrillary acidic protein (GFAP) antibody (1:1000; Sigma), then incubated at room temperature for 1–2 h with Cy2-conjugated anti-mouse IgG (1:200; Jackson), and Cy3-conjugated anti-rabbit IgG antibody (1:200; Jackson). For endothelial cell detection, the sections were labeled with Alexa Fluor 488-conjugated lectin B4 (IB4; Invitrogen, Carlsbad, CA, USA). After washing in PBS, the sections were mounted on an MAS-coated glass slide and examined for fluorescent signals using a confocal laser-scanning microscope (FV1000; Olympus, Tokyo, Japan). BrdU-labeled cells throughout the rostro-caudal extent of the DG were counted in every sixth section, and the total number of BrdU-labeled cells was calculated by multiplying the count (Maekawa et al., 2005).

Reverse transcription-PCR (RT-PCR)

Total RNA was extracted from the dissected DG or neurospheres prepared from P1 hippocampus using an RNeasy Plus Mini kit (QIAGEN, Germantown, ML, USA), and cDNA was synthesized using an Advantage RT-for-PCR kit (Clontech, Palo Alto, CA, USA) according to the manufacturer's instructions. PCR was performed using Ex Taq (Takara, Shiga, Japan) and a thermal cycler (Verti; Applied Biosystems, Foster City, CA, USA). The primers, annealing temperatures, and sizes of the PCR products are shown in Table 1. The thermocycle conditions were as follows: 30 s at 98 °C, 50 s at the annealing temperature (Table 1), 40 s at 72 °C for 30 cycles (BDNF, FGF-2, VEGF and PEDF), and 45 cycles (EGF) or 25 cycles (glyceraldehydes-3-phosphate dehydrogenase (GAPDH), which was used as an internal control).

A real-time PCR analysis was performed using the SYBER green labeling system (SYBER Premix Ex Taq 2; Takara) and the ABI Prism 7700 Sequence Detection System (Applied Biosystems). Amplifications were carried out in a 96-well optical plate, and the thermocycle conditions were as follows: 5 s at 95 °C, 10 s at 55 °C, and 30 s at 72 °C for 40 cycles. A quantitative analysis was performed using the delta-delta Ct method with GAPDH as an internal control (Kodomari et al., 2009).

Immunoblot analysis

Cell lysate was prepared from the dissected DG at 2 days after the injection of memantine or saline, as described previously (Hattori et al., 2006). Briefly, the dissected DG was homogenized in lysis buffer (10 mM Tris–HCl (pH 7.5), 150 mM NaCl, 1 mM EDTA, 1% Triton X-100, 0.1% sodium deoxycholate, 0.1% SDS, and protease inhibitor cocktail (Roche Diagnostics, Mannheim, Germany)

Table 1. Primer sequences for PCR

Name	Forward primer (5′–3′)	Reverse primer (5′–3′)	Condition (°C)	Amplification size (bp)	Accession No.
BDNF	GGACTCTGGAGAGCGTGAAT	GTCCTCATCCAGCAGCTCTT	55	107	NM_007540
EGF	AGAGCCAGTTCAGTAGAAACTGGG	ACTTTGGTTTCTAATGATTTTCTCC	55	256	NM_010113
FGF-2	AACCGGTACCTTGCTATGAAG	GTTCGTTTCAGTGCCACATAC	55	152	NM_008006
GAPDH	GTCATCATCTCCGCCCCTTCTGC	GATGCCTGCTTCACCACCTTCTTG	55	443	NM_008084
PEDF	GGCAGTGGGTAACCAAGTTTG	GCAGCTGGGCAATCTTGCAG	55	156	NM_011340
VEGF	GACACACCCACCCACATACA	AAAGGACTTCGGCCTCTCTC	60	247	NM_001025250

using a Polytoron homogenizer. After removing the insoluble material by centrifugation (2000×*g*, 4 °C, 10 min), the protein concentration in the supernatant was determined using BCA protein assay reagent (Pierce, Rockford, IL, USA).

The proteins were separated by electrophoresis using an SDS polyacrylamide gel (SuperSep 15–20%; Wako Pure Chemical Industries, Osaka, Japan) and then electrophoretically transferred to a nitrocellulose membrane (Immobilon; Millipore, Bedford, MA, USA). The membrane was blocked by incubation at room temperature for 1 h with 5% skim milk in Tris-buffered saline containing 0.1% Tween 20 (TBST) and then incubated at 4 °C overnight with mouse monoclonal anti-human PEDF antibody (1:500; Trans Genic Inc., Hyogo, Japan). After washing in TBST, the membrane was incubated with horseradish peroxidase-conjugated anti-rabbit IgG secondary antibody (1:1000; Sigma) at room temperature for 1 h. Immunoreactive bands were visualized using a chemiluminescence detection system (ECL; Amersham Biosciences, Piscataway, NJ, USA). The membrane was then incubated with Stripping buffer (62.5 mM Tris–HCl (pH 7.5), 2% SDS, 100 mM 2-mercaptoethanol) at 60 °C for 30 min, blocked with 3% skim milk in TBST, re-probed with anti-β actin antibody (1:1000; Sigma), and then incubated with horseradish peroxidase-conjugated anti-rabbit IgG secondary antibody (1:1000; Sigma). The density of the bands was measured using NIH ImageJ software. Each sample was normalized with the density of the β-actin signal.

Preparation of neurospheres and immunocytochemistry

Neurospheres were prepared from the hippocampus of P1 mouse as described previously (Walker et al., 2008). Briefly, the hippocampus was dissected, filtered through Cell Strainer (BD Falcon 40 μm; BD Biosciences, Bedford, MA, USA), and centrifuged at 1000 rpm for 5 min. The pellet was suspended in neurosphere growth medium (mouse NeuroCult NSC Basal Medium plus mouse NeuroCult NSC Proliferation Supplements) (Stem Cell Technologies, Vancouver, BC, Canada) with 2 μg/ml heparin (Sigma), 20 ng/ml purified mouse receptor grade EGF (Roche Diagnostics) and 10 ng/ml recombinant bovine FGF-2 (Roche Diagnostics). The cells were plated at a density of 2×10^4 cells/ml in a 12-well plate (Corning, Corning, NY, USA) and incubated at 37 °C under an atmosphere of humidified 5% CO_2 for the indicated periods. Recombinant human PEDF was prepared from *Escherichia coli* expressing human PEDF as described previously (Yabe et al., 2005) and added to the growth medium of neurospheres at a concentration of 25 ng/ml. To generate secondary neurospheres, primary neurospheres at DIV7 were harvested, dissociated and then plated at a density of 2×10^4 cells/ml in a 12-well plate (Corning). The cells were incubated for 5 days in neurosphere growth medium with heparin, EGF and FGF-2 but without PEDF.

For the cellular proliferation assay, the neurospheres were cultured for 4 days in neurosphere growth medium, incubated in the presence or in the absence of 25 ng/ml PEDF for 12 h and subsequently maintained with 1 μM BrdU for 2 h. The neurospheres were then dissociated and collected by centrifugation (900 rpm, 5 min). The pellet was suspended in 4% PFA for 5 min and the cells were mounted onto an MAS-coated glass slide. The cells were washed with PBS and incubated in 2N HCl at 37 °C for 35 min. After washing in PBS, they were incubated with anti-BrdU antibody (1:400) at 4 °C for 1 h in PBS containing 1% BSA and 0.1% Triton X-100. After washing in PBS, they were then incubated at room temperature for 1–2 h in PBS containing 1% BSA plus Cy3-conjugated anti-rat IgG antibody (1:200) and Hoechst, and examined for fluorescent signals using a fluorescence microscope (AX70; Olympus, Tokyo, Japan). To examine the cellular proliferation using an anti-phosphorylated histone H3 antibody, the neurospheres were immunostained with mouse monoclonal anti-phosphorylated histone H3 antibody (1:200; Cell Signaling Technology, Danvers, MA, USA) and Cy3-conjugated anti-mouse IgG antibody (1:200) according to the immunocytochemical method described above.

For the cell differentiation assay, the neurospheres were plated onto poly-L-lysine-coated coverslips in NeuroCult NSC Basal Medium containing mouse NeuroCult NSC Proliferation Supplements and 2% fetal calf serum without EGF and FGF-2 and were cultured for 5 days. The differentiated cells were incubated with mouse monoclonal anti-O4 antibody (1:100, Chemicon) at 37 °C for 1 h, washed with PBS, and then fixed with 4% PFA at room temperature for 10 min. After washing in PBS, they were incubated with rabbit polyclonal anti-GFAP antibody (1:800; Dako, Glostrup, Denmark) and goat polyclonal anti-doublecortin (Dcx) antibody (1:400; Santa Cruz Biotechnology, Santa Cruz, CA, USA) at 4 °C for 1 h in PBS containing 1% BSA and 0.1% Triton X-100. After washing in PBS, the cells were then incubated at room temperature for 1–2 h in PBS containing 1% BSA plus Cy5-conjugated anti-rabbit IgG antibody (1:200), Cy3-conjugated anti-goat IgG antibody (1:200), and Cy2-conjugated anti-mouse IgM antibody (1:200). The fluorescent signals were examined using a confocal laser-scanning microscope (FV1000).

Infection of adeno-associated virus (AAV) into dentate gyrus *in vivo*

AAV carrying mouse PEDF cDNA (mPEDF) was prepared according to the manufacturer's instructions. Briefly, FLAG-tagged mPEDF cDNA (Hosomichi et al., 2005) was cloned into the plasmid pAAVMCS under CMV promoter (Stratagene, La Jolla, CA, USA) (pAAVMCS-mPEDF). HEK293 cells were transfected with pAAVMCS-mPEDF or pAAVMCS-EGFP (Yasuda et al., 2007) using Lipofectamine 2000 reagent (Invitrogen). The cells were harvested at 48 h after the transfection, and then AAV was purified by ultracentrifugation (13,000×*g*, 4 °C, 18.5 h). To confirm the expression of mPEDF, COS7 cells were infected with AAV-mPEDF or AAV-EGFP. The cultured medium was collected 48 h after the infection, and then the expression of mPEDF was checked by immunoblotting using mouse monoclonal anti-FLAG antibody (1:1000; Sigma) (Fig. 7A). The AAV-mPEDF and AAV-EGFP (0.95+0.05 μl/injection) or the AAV-EGFP (1 μl/injection) as a control was stereotaxically injected into the DG (anteroposterior, 2.5 mm; lateral, 2.0 mm; ventral, 3.0 mm from bregma, respectively) as described previously (Seki et al., 2007).

Statistical analysis

Data were evaluated using a one-way analysis of variance followed by a post-hoc Scheffé *F*-test. All values were expressed as the mean±SEM, and *P*-values less than 0.05 were considered significant.

RESULTS

Memantine increases cellular proliferation in adult hippocampus

To investigate the effect of memantine on cellular proliferation in adult hippocampus, we injected the mice with a dose of 10, 30, and 50 mg/kg of memantine followed by the injection of BrdU 3 days thereafter. The brains were then fixed 1 day later; after preparing the brain sections, we immunostained them with anti-BrdU antibody, and then counted the number of BrdU-labeled cells. The number of BrdU-labeled cells was significantly increased at a dose of 50 mg/kg of memantine (Fig. 1A; control: 3476.0±149.9 cells/DG, n=4, 10 mg/kg: 3204.0±210.9 cells/DG, n=4, 30 mg/kg: 3137.0±137.2 cells/DG, n=4, 50 mg/kg: 8103.0±

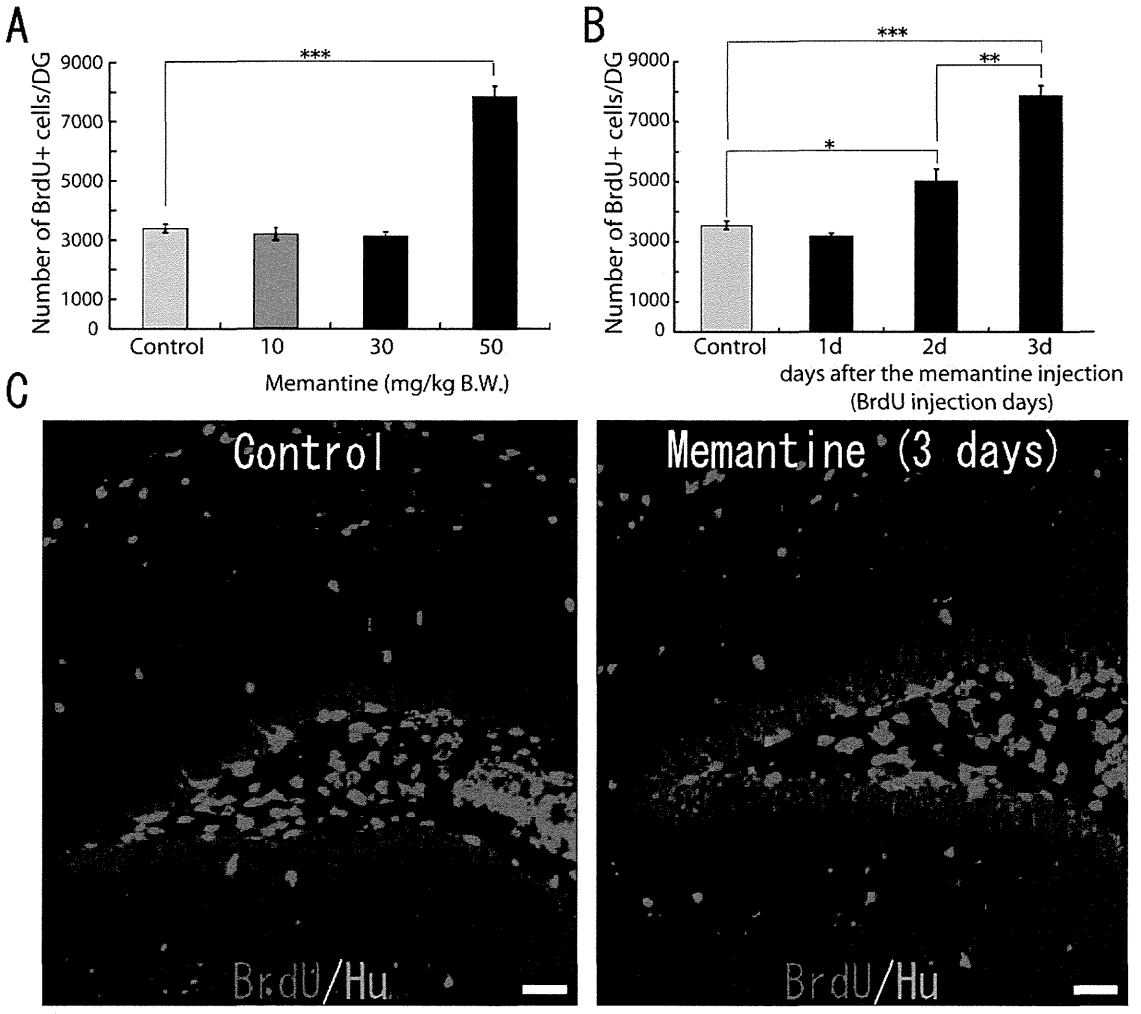

Fig. 1. Effect of memantine on cellular proliferation in the GCL. (A) Dose effect of memantine on cellular proliferation in the GCL. Three-month-old mice were injected i.p. with a dose of 10, 30, 50 mg/kg memantine and injected i.p. with BrdU one day after the memantine-injection. The brains were fixed 3 days after the BrdU-injection, stained with anti-BrdU antibody and the BrdU-labeled cells were counted. *** $P<0.000\,001$. (B) Temporal effect of memantine on cellular proliferation in the GCL. Three-month-old mice were injected i.p. with a dose of 50 mg/kg memantine and injected i.p. with BrdU 1, 2, or 3 days after the memantine-injection. The brains were fixed one day after BrdU-injection, stained with anti-BrdU antibody and the BrdU-labeled cells were counted. * $P<0.05$, ** $P<0.001$, *** $P<0.000\,001$. Error bars indicate standard error of the mean. (C) Representative examples of BrdU-labeled cells (red) in the control group (left panel) and the memantine-injected group (right panel). The sections were co-stained with Hoechst (blue). Scale bars=50 μm.

321.6 cells/DG, $n=4$). Next, to investigate the temporal effect of memantine, we injected the mice with a dose of 50 mg/kg of memantine followed by the injection of BrdU 1, 2 or 3 days thereafter. The brains were then fixed 1 day after each BrdU-injection; after preparing the brain sections, we immunostained them with anti-BrdU antibody, and then counted the number of BrdU-labeled cells. The number of BrdU-labeled cells gradually increased after the injection of memantine (Fig. 1B, C; control: 3393.6±142.4 cells/DG, $n=5$, 1 day after memantine-injection: 3160.0±122.7 cells/DG, $n=3$, 2 days after memantine-injection: 5001.3±420.7 cells/DG, $n=3$, 3 days after memantine-injection: 7851.2±354.2 cells/DG, $n=5$). These results indicate that memantine increases cellular proliferation in adult hippocampus.

To examine whether the memantine directly affects proliferation of progenitor cells using neurospheres prepared from neonatal mouse hippocampus, we initially confirmed that memantine-treatment increased the number of BrdU-labeled cells in the neonatal hippocampus *in vivo* as well as in the adult hippocampus (Fig. 2B, C; control: 12504.0±874.0 cells/DG, $n=3$, 50 mg/kg: 16876.0±499.4 cells/DG, $n=3$, $P<0.05$). Neurospheres were cultured for 7 days in the presence or in the absence (control) of 1 μM memantine, and the numbers of the large size of primary neurospheres (more than 100 μm in diameter) and the small size of neurospheres were counted (Fig. 2D, E; memantine: 44.2±3.2 large size of neurospheres/well and 132.2±13.4 small size of neurospheres/well, $n=5$, control: 48.8±3.5 large size of neurospheres/well and 137.4±13.7 small size of neurospheres/well, $n=5$). These results indicate that these are no significant differences in the number of both sizes of neurospheres in between memantine-treated and untreated cultures, suggesting that memantine fails to affect directly proliferation of the hippocampal progenitor cells.

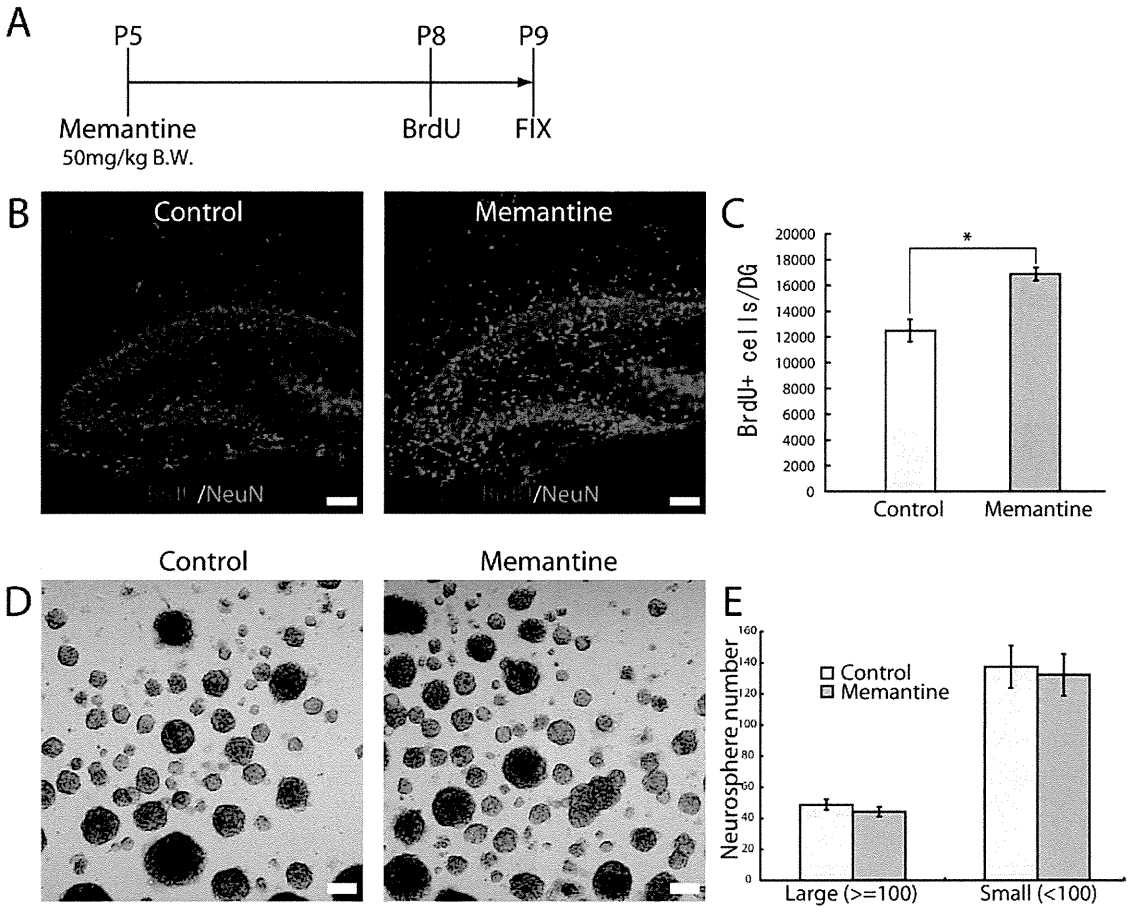

Fig. 2. Effect of memantine on cellular proliferation of hippocampal progenitor cells *in vivo* and *in vitro*. (A) Schematic illustration of the *in vivo* experimental design. (B) Representative examples of BrdU-labeled cells (red) in the DG. P5 mice were injected i.p. with a dose of 50 mg/kg memantine, and with BrdU 3 days after the memantine-injection. The brains were fixed one day after the BrdU-injection and stained with anti-BrdU antibody. The sections were co-stained with Hoechst (blue). (C) Quantitative analysis of the number of BrdU-positive cells in the DG. * $P<0.05$. (D) Primary neurosphere formation. Neurospheres prepared from P1 mouse hippocampus were cultured for 7 days in the absence (control) or in the presence of 1 μM memantine. (E) Quantitative analysis of the number of neurospheres. Scale bars=50 μm in panel B and 100 μm in panel D. Error bars indicate standard deviation.

Memantine up-regulates PEDF expression in adult hippocampus

To search for a factor that mediates the memantine-induced increase in cellular proliferation, we used RT-PCR to investigate gene expression in the DG of memantine-injected mice (50 mg/kg i.p.) and saline-injected (control) mice 1 day after the injection of memantine or saline. We found that the expressions of BDNF, FGF-2 and PEDF were clearly increased after the injection of memantine, whereas the expression levels of EGF and VEGF were not significantly changed (Fig. 3A). Since previous studies showed that neither BDNF nor FGF-2 stimulated the cell proliferation of neural progenitor cells in adult hippocampus (Kuhn et al., 1997; Walker et al., 2008), we here examined the effect of memantine on the expression of PEDF by using real-time PCR technique. The expression of PEDF mRNA was significantly increased 1, 2 and 3 days after memantine-injection (1 day: 3.46-fold, $P=0.0014$, 2 days: 3.51-fold, $P=0.0022$, 3 days: 2.66-fold, $P=0.040$, $n=3$ animals per each group) (Fig. 3B). The expression level of PEDF protein was also increased by 1.79-fold ($n=3$) 2 days after the injection of memantine (Fig. 4A, B). An immnohistochemical study using anti-PEDF antibody showed the prominent expression of PEDF in the hippocampal fissure, the molecular layer, hilus and subgranular zone (SGZ) of the DG (Fig. 4C–F). These results indicate that memantine up-regulates PEDF expression in the DG. In addition, most of the cells expressing PEDF in the molecular layer were positive for anti-GFAP antibody, suggesting that the majority of the PEDF-expressing cells were protoplasmic astrocytes (Fig. 4D) and perivascular astrocytes (Fig. 4E).

PEDF stimulates cellular proliferation of hippocampal progenitor cells *in vitro*

We next investigated the effect of PEDF on cellular proliferation using a neurosphere assay. When neurospheres prepared from P1 mouse hippocampus were cultured for 7 days in the absence (control) or presence of PEDF (25 ng/ml) together with EGF and FGF-2, the number of large

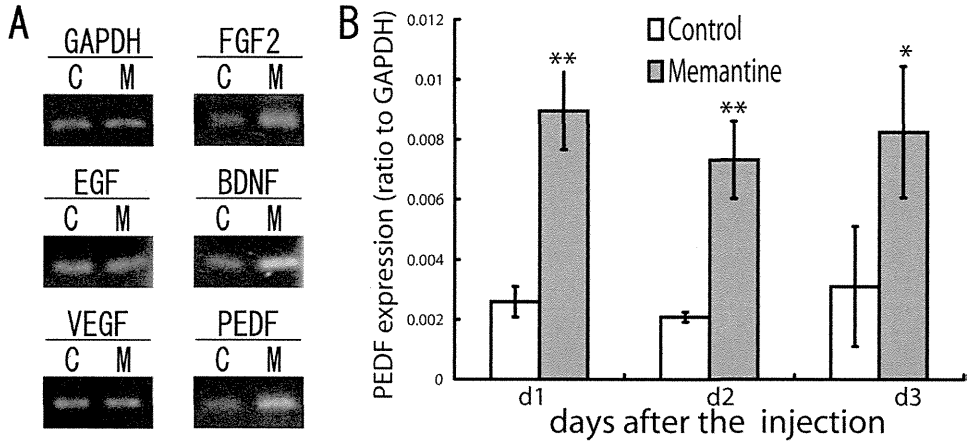

Fig. 3. Increased expression of PEDF mRNA in the DG after the injection of memantine. (A) RT-PCR analysis. Total RNA was prepared from the dissected DG of saline-injected mice (C; control) or mice injected with 50 mg/kg of memantine (M). (B) Temporal analysis of PEDF mRNA expression. The ratio of PEDF mRNA expression (PEDF/GAPDH) was evaluated using a real-time PCR analysis. * $P<0.05$, ** $P<0.001$. Error bars indicate standard deviation.

primary neurospheres increased by 1.6-fold ($n=12$), whereas no significant differences in the number of small neurospheres were observed ($n=12$) (Fig. 5A, B). On the other hand, when the neurospheres were cultured without EGF and FGF-2, no large neurospheres were observed, even in the presence of PEDF (data not shown). It has been generally considered that large neurospheres are derived from self-renewing progenitor cells and small neurospheres are generated from progenitor cells that have more restricted self-renewal ability (Seaberg and van der Kooy, 2002). To evaluate the effect of PEDF on the self-renewal ability of progenitor cell, primary neurospheres cultured with or without PEDF (25 ng/ml) were dissociated and maintained without PEDF for 5 days to generate secondary neurospheres. The number of the large secondary neurospheres significantly increased by 1.5-fold ($n=5$) (Fig. 5C, D), suggesting that PEDF stimulates the self-renewal of progenitor cells. We next analyzed the effect of PEDF on the proliferation of progenitor cells. Using primary neurospheres, we performed a BrdU-incorporation assay and anti-phosphorylated histone H3 antibody staining. Primaly neurospheres cultured for 4 days were incubated with or without PEDF (25 ng/ml) for 12 h and were subsequently incubated with BrdU for 2 h. PEDF treatment increased the percentages of BrdU-labeled cells (Fig. 5E, F; PEDF: 42.9±3.3%, control: 21.0±1.8%, $n=4$) and phosphorylated histone H3-positive cells (Fig. 5G, H; PEDF: 11.5±2.2%, control: 4.0±0.8%, $n=4$) among the neurosphere-forming cells.

We next examined the effect of PEDF on cellular differentiation as evaluated using anti-Dcx antibody, anti-GFAP antibody and anti-O4 antibody staining. Primary neurospheres were dissociated and plated onto PLL-coated coverslips, cultured for 7 days with or without PEDF (25 ng/ml), and then allowed to differentiate by culturing for 5 days in a medium without growth factors. Since no significant differences in the percentage of neuron (Dcx+), astrocyte (GFAP+) and oligodendrocyte (O4+) after PEDF-treatment were observed (Fig. 6A, B), we confirmed that PEDF hardly affected cellular differentiation. We further investigated the effect of PEDF on multipotency of neurospheres under the clonal condition. The percentage of three types of neural lineages; Dcx/GFAP/O4, Dcx/GFAP, and GFAP, was almost similar between control and PEDF-treated neurosheres (Fig. 6C). These results suggest that PEDF enhances cellular proliferation and self-renewing but is not involved in the multilineage potency of hippocampal progenitor cells.

We next examined the effect of PEDF on cellular proliferation of hippocampal progenitor *in vivo*. AAV carrying mouse PEDF and EGFP cDNAs or carrying EGFP cDNA alone as a control was infected into the DG. The mice were injected i.p. with BrdU 7 days after the AAV-infection, and fixed 1 day after the BrdU-injection. However, there were no significant differences in the number of the BrdU-labeled cells in the granule cell layer (GCL) between PEDF-infected group and control group (Fig. 7), suggesting that PEDF *per se* does not stimulate the cellular proliferation.

DISCUSSION

Recent studies have shown that memantine promotes cellular proliferation and the production of mature granule cells in adult hippocampus (Jin et al., 2006; Maekawa et al., 2009). However, the molecular mechanism responsible for the memantine-induced promotion of cellular proliferation remains unknown. Marvanova et al. (2001) reported that memantine at a dose of 50 mg/kg, the same dose used in our study, clearly induced the expression of BDNF and its receptor TrkB in adult hippocampus, similar to our results (Fig. 3), but recent studies have revealed that BDNF signaling mainly acts on the survival of newly generated cells, rather than cellular proliferation (Sairanen et al., 2005). Additionally BDNF signaling did not affect the proliferation of hippocampal progenitor cells, unlike SVZ progenitor cells, in an *in vitro* experiment (Walker et al., 2008). Furthermore, FGF-2, a mitogen for neural stem cells in *in vitro* experiments (Reynolds and Weiss, 1992),

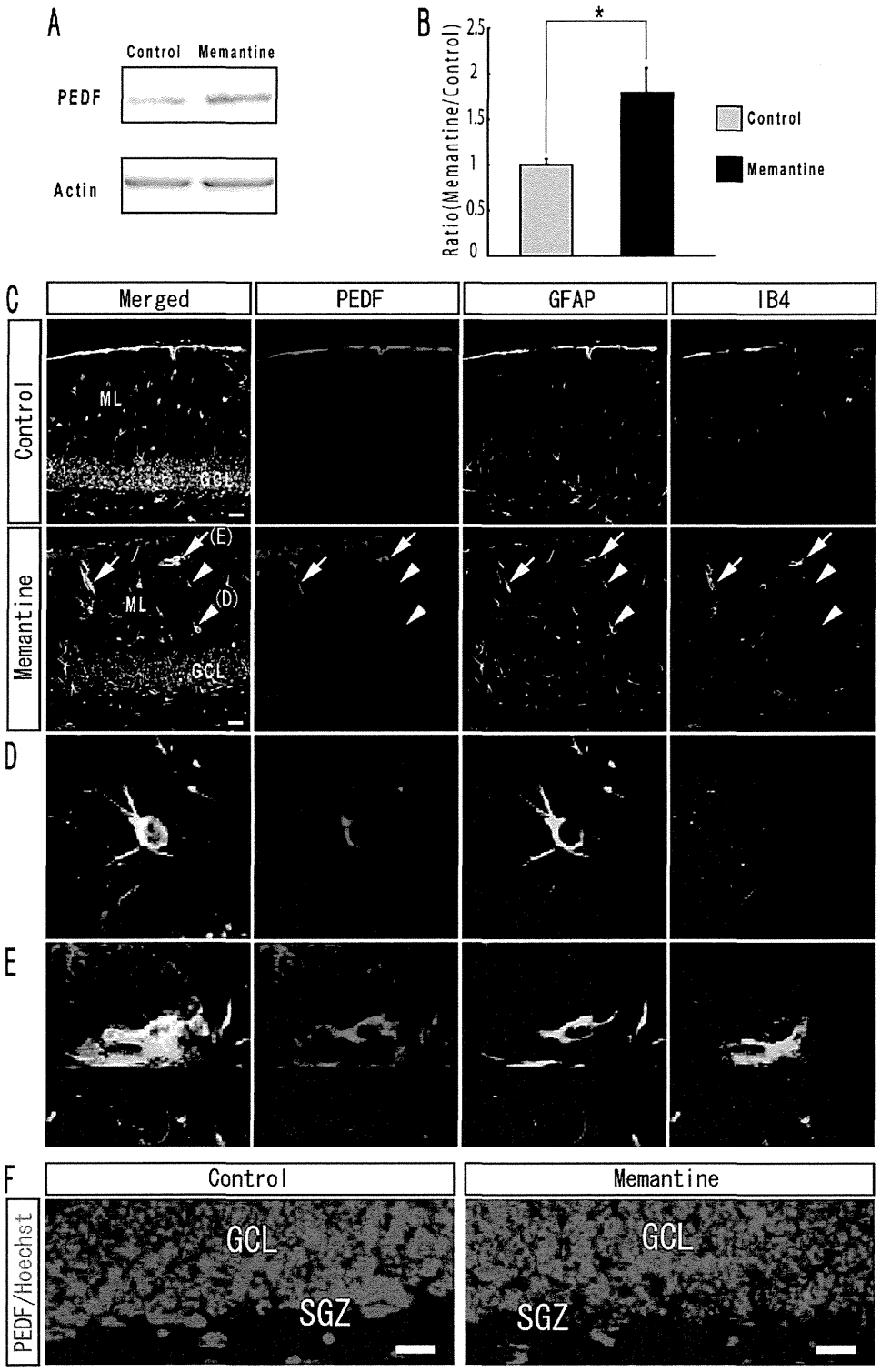

Fig. 4. Up-regulation of PEDF expression in the DG after the injection of memantine. (A) Immunoblot analysis. Three-month-old mice were injected i.p. with a dose of 50 mg/kg memantine, and cell lysate was prepared from the DG 2 days after the memantine-injection. Protein samples (30 μg) were separated using SDS-PAGE and immunoblotted with anti-PEDF antibody and ant-actin antibody as an internal control. (B) Quantitative analysis of PEDF protein expression. The ratio of PEDF protein expression (memantine-injected group/control group) was evaluated using an immunoblot analysis. * $P<0.05$. Error bars indicate standard error of the mean. (C–F) Immunohistochemical analysis. Three-month-old mice were injected i.p. with a dose of 50 mg/kg memantine, and the brains were fixed 2 days after memantine-injection. Representative examples of PEDF-positive cells (red), GFAP-positive cells (blue), and IB4-positive cells (green) in the DG at a lower magnification (C) and higher magnification (D, E). The arrows indicate endothelial cells and the arrowheads indicate astrocyte. GCL, granule cell layer; ML, molecular layer. (F) Representative examples of PEDF-positive cells (red) in the SVZ at a higher magnification. The sections were co-stained with Hoechst (blue). SGZ, subgranular zone. Scale bars=20 μm in panels C and F.

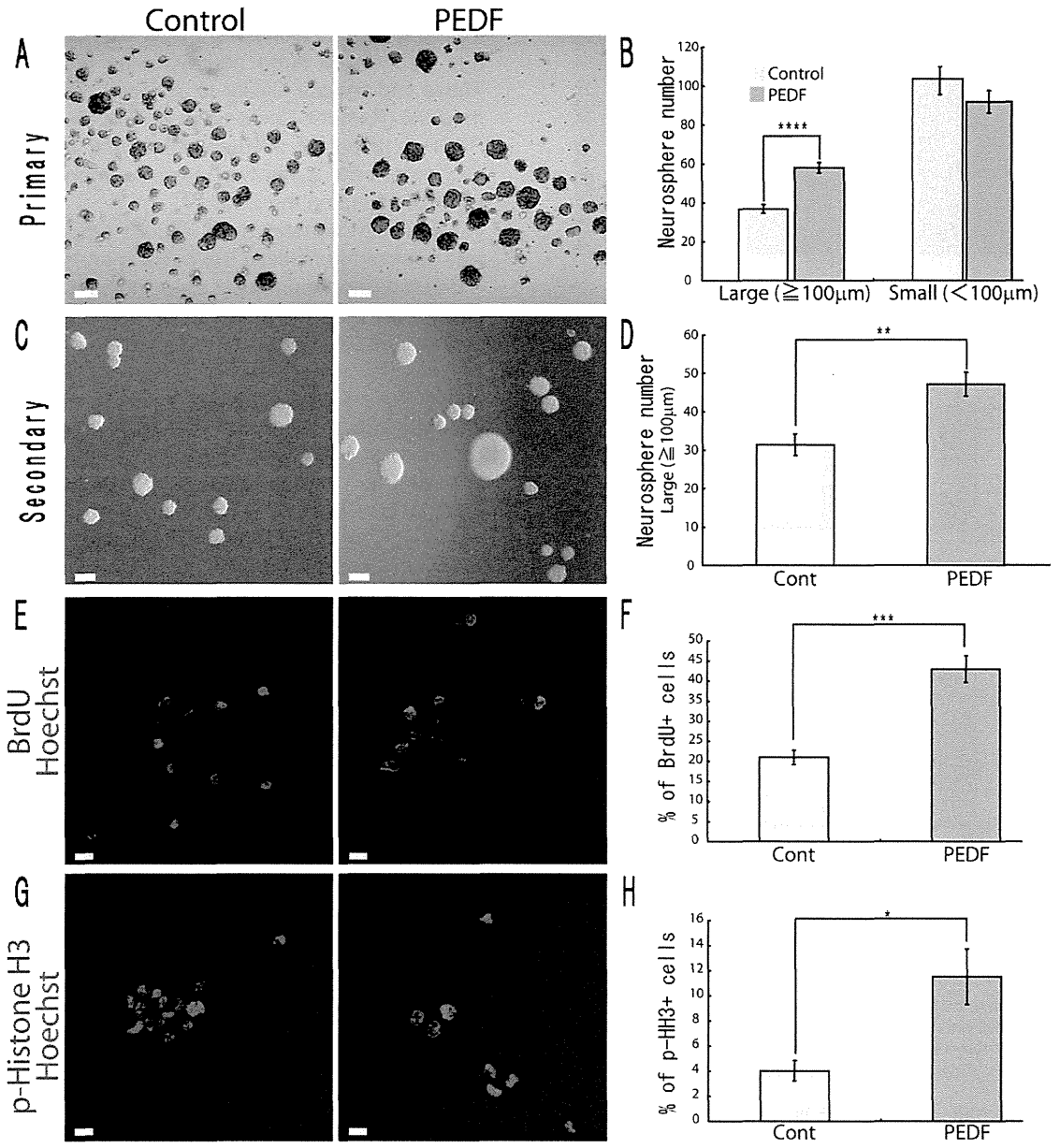

Fig. 5. Effects of PEDF on neurosphere formation, proliferation and differentiation of hippocampal progenitor cells. (A) Primary neurosphere formation. Neurospheres prepared from P1 mouse hippocampus were cultured for 7 days in the absence (control) or in the presence of PEDF (25 ng/ml). (B) Quantitative analysis of the number of primary neurospheres. (C) Secondary neurosphere formation. Primary neurospheres were generated in the absence (control) or in the presence of PEDF (25 ng/ml), passaged and then cultured for 5 days to generate secondary neurospheres. (D) Quantitative analysis of the number of secondary neurospheres. (E, G) Immunocytochemical experiments. Neurospheres cultured for 4 days were maintained in the absence (control) or in the presence of PEDF (25 ng/ml) for 12 h, and subsequently incubated with BrdU for 2 h. After washing, they were immunostained with anti-BrdU antibody (red in E) or anti-phosphorylated histone H3 (p-Histone H3) antibody (red in G). The cells were co-stained with Hoechst (blue). (F, H) Quantitative analysis of the percentage of BrdU-labeled cells (F) and p-Histone H3-positive cells (H). * $P<0.05$, ** $P<0.01$, *** $P<0.001$ and **** $P<0.00001$, when compared with the control culture. Scale bars=100 μm in panels A and C, 10 μm in panels E and G. Error bars indicate standard error of the mean.

was also up-regulated by the injection of memantine in adult hippocampus (Fig. 3 and Namba et al., 2009). *In vivo* experiments, however, have showed that FGF-2 failed to stimulate the proliferation of hippocampal progenitor cells in the young adult mice (Kuhn et al., 1997; Wagner et al., 1999; Jin et al., 2003). Therefore, distinct factors likely mediate the effect of memantine on cellular proliferation in adult hippocampus. In the present study, we found that the expression of PEDF was dramatically increased by the injection of memantine in adult hippocampus. PEDF was initially identified as a differentiating factor for retinoblastoma cells (Tombran-Tink et al., 1991), and later studies have shown that it also has neurotrophic and neuroprotective functions in various neuronal populations, as well as

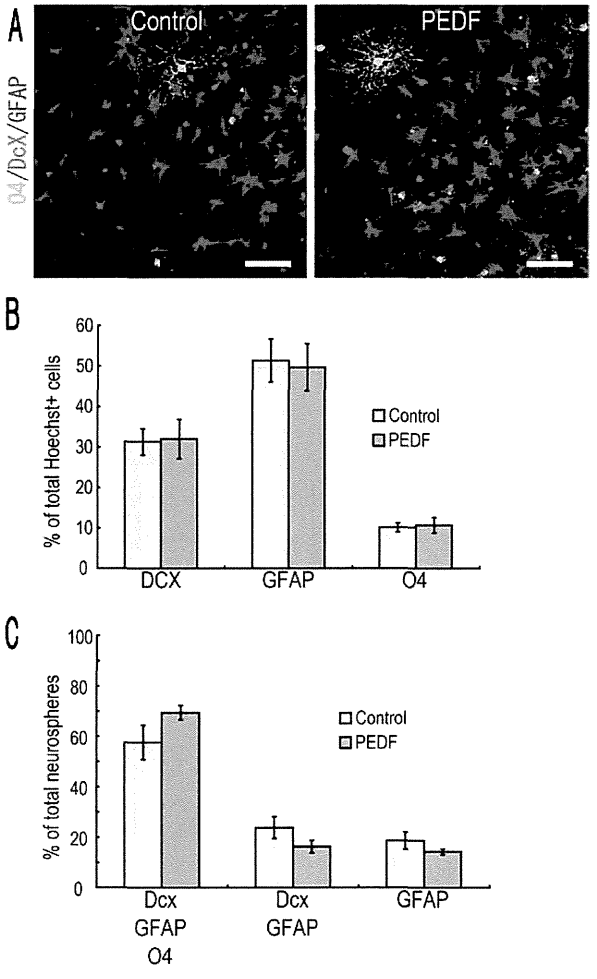

Fig. 6. Differentiation of hippocampal progenitor cells. (A) Representative immunohistochemical staining with anti-O4 antibody (green), anti-Dcx antibody (red) and anti-GFAP antibody (blue). Scale bars=50 μm. (B) Quantitative analysis of the percentage of Dcx-positive cells, GFAP-positive cells and O4-positive cells. (C) Quantitative analysis of the percentage of three types of neural lineages; Dcx/GFAP/O4, Dcx/GFAP, and GFAP. Error bars indicate standard error of the mean.

acting as a potent anti-angiogenic factor (Tombran-Tink and Barnstable, 2003; Sanagi et al., 2008). Interestingly, recent studies have shown that the expression of PEDF is increased by ischemic insult and antidepressant treatment (Miller et al., 2008; Sanagi et al., 2008). Neurogenesis is known to be enhanced under these conditions (Malberg et al., 2000; Tanaka et al., 2004). Furthermore, Ramirez-Castillejo et al. (2006) reported that PEDF increased the number of neurospheres derived from adult SVZ but did not affect the average size of the neurospheres. In the present study using hippocampal neurospheres, we also showed that PEDF increased the number of large neurospheres and enhanced the proliferation of progenitor cells in the presence of EGF and FGF-2 but did not stimulate their proliferation in the absence of EGF and FGF-2. In accordance with the results of *in vitro* study, PEDF expressed by using AAV did not stimulate the cellular proliferation *in vivo*. These results suggest that PEDF is an enhancing molecule for the proliferation of hippocampal progenitor cells in the presence of mitogens such as FGF-2 and EGF. Moreover, PEDF did not affect the average size of the large neurospheres (data not shown). These findings are similar to previous results obtained in the SVZ (Ramirez-Castillejo et al., 2006), suggesting that PEDF is a potent microenvironmental factor for neural progenitor cells in the two major neurogenic regions: the hippocampus and the SVZ.

Ramirez-Castillejo et al. (2006) reported that PEDF was released from lectin IB4-positive endothelial cells and S100β-positive ependymal cells in the SVZ but not expressed by SVZ progenitor cells. Furthermore, PEDF increased the expression of Notch effectors Hes1 and Hes5 in neuronal progenitor cells (Ramirez-Castillejo et al., 2006). Our previous study using the neocortices of mouse embryos also showed that an NMDA receptor antagonist promoted the proliferation of progenitor cells in the SVZ and increased the expression of Hes1 and Hes5 (Hirasawa et al., 2003). In the hippocampus, however, an immunohistochemical study demonstrated that PEDF was expressed in the GFAP-positive protoplasmic and perivascular astrocytes (Fig. 4) and hippocampal progenitor cells *in vitro* (data not shown), and neither increases in the expression of Hes1 nor Hes5 were detected after the injection of memantine (data not shown). Thus, the mechanism by which PEDF increases the proliferation of progenitor cells might differ between the hippocampus and the SVZ.

Memantine has been used clinically as a neuroprotective agent to treat moderate-to-severe Alzheimer's disease (AD). In clinical practice, a stable dose of memantine (20 mg/day) has been found to produce a steady-state plasma memantine level of approximately 0.5 μM in AD patients (Kornhuber and Quack, 1995). In rodent, the oral administration of memantine (30 mg/kg daily for 5 weeks) produced a steady-state plasma memantine concentration of $\sim$1 μM, and it improved spatial learning in a transgenic mouse model of AD (Minkeviciene et al., 2004). In addition, the administration of memantine by an intragastric route (7.5 mg/kg daily for 2 weeks) increased the proliferation of progenitor cells in the hippocampus (Jin et al., 2006). Interestingly, a higher oral dose of memantine (100 mg/kg daily for 4 weeks), which produced a steady-state plasma memantine concentration of approximately 6 μM (>10-fold higher than clinical level), improved cognition and had a potential anxiolytic response in mice (Minkeviciene et al., 2008), suggesting that the different ranges of memantine dose result in different pharmacological effects although adverse effects in rodent have not been elucidated. By contrast, in case of an acute administration of memantine such as by i.p. injection, since a 2.5–5.0 mg/kg dose of memantine produced a plasma memantine concentration of approximately 1 μM (Danysz et al., 1997), the 50 mg/kg i.p. dose of memantine used in our experiments likely produced a higher plasma memantine concentration (probably >10-fold higher than the concentration of a therapeutic dose), and we found that only higher dose of memantine increased both the proliferation of progenitor cells and the expression level of PEDF. To elucidate the molecular mechanism responsible for memantine-in-

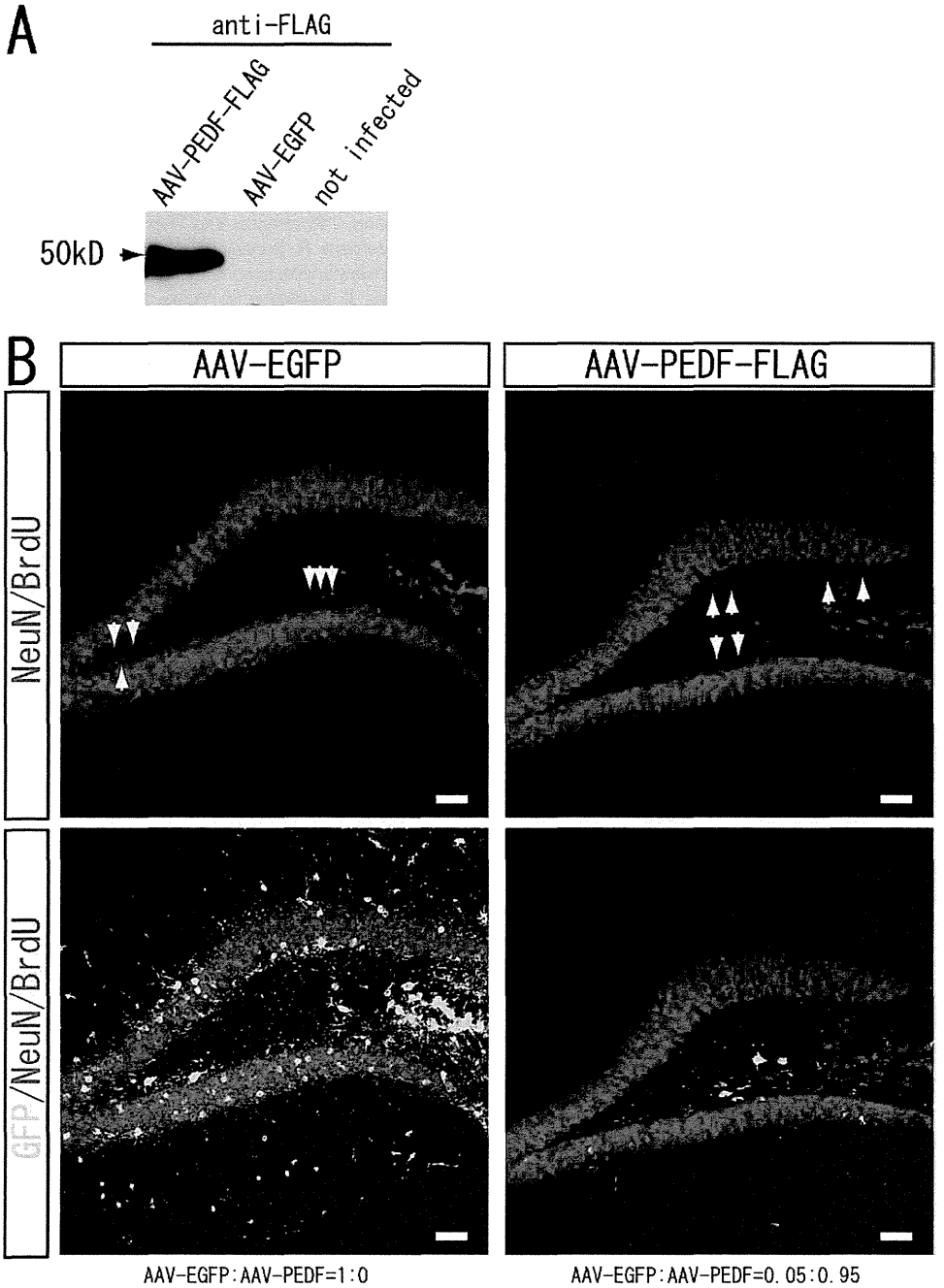

Fig. 7. Effect of PEDF on cellular proliferation in the DG. (A) Immunoblotting with anti-FLAG antibody. AAV-mPEDF or AAV-GFP was infected into COS7 cells, and equal amounts of culture media were subjected to immunoblot analysis. (B) Representative examples of BrdU-labeled cells (red) shown by arrowheads. Three-month-old mice were infected with AAV-mPEDF and AAV-EGFP or AAV-EGFP alone, and then injected i.p. with BrdU 7 days after the AAV-infection. The mice were fixed one day after the BrdU-injection. The sections were co-stained with anti-NeuN antibody (blue). AAV-infected cells were visualized by EGFP signals. Scale bars=50 μm.

duced PEDF up-regulation, we will need further studies including the investigation of PEDF expression under the same condition as clinical practice.

CONCLUSION

In conclusion, to clarify the molecular bases of the promotion of cell proliferation by memantine, we searched for a factor that mediates memantine-induced cellular proliferation, and found that PEDF is up-regulated in the DG of adult mice after the memantine-injection. Using neurosphere assay we confirmed that PEDF enhanced the cellular proliferation but was not involved in the multilineage potency of hippocampal progenitor cells. Since present and previous studies have shown that neither PEDF nor